POTSDAM-INSTITUT FÜR
KLIMAFOLGENFORSCHUNG

Effects of parameter uncertainties on the modeling of terrestrial biosphere dynamics

S. Zaehle and S. Sitch[1]

Department of Global Change and Natural Systems, Potsdam Institute for Climate Impact Research (PIK), Potsdam, Germany

B. Smith

Physical Geography and Ecosystems Analysis, Geobiosphere Science Centre, Lund University, Lund, Sweden

F. Hatterman

Department of Global Change and Natural Systems, Potsdam Institute for Climate Impact Research (PIK), Potsdam, Germany

Received 25 October 2004; revised 31 May 2005; accepted 22 June 2005; published 14 September 2005.

[1] Dynamic global vegetation models (DGVMs) have been shown to broadly reproduce seasonal and interannual patterns of carbon exchange, as well as realistic vegetation dynamics. To assess the uncertainties in these results associated with model parameterization, the Lund-Potsdam-Jena-DGVM (LPJ-DGVM) is analyzed in terms of model robustness and key sensitive parameters. Present-day global land-atmosphere carbon fluxes are relatively well constrained, despite considerable uncertainty in global net primary production mainly propagating from uncertainty in parameters controlling assimilation rate, plant respiration and plant water balance. In response to climate change, water-use efficiency driven increases in net carbon assimilation by plants, transient changes in vegetation composition and global warming effects on soil organic matter dynamics are robust model results. As a consequence, long-term trends in land-atmosphere fluxes are consistently modeled despite an uncertainty range of -3.35 ± 1.45 PgC yr^{-1} at the end of the twenty-first century for the specific scenario used.

Citation: Zaehle, S., S. Sitch, B. Smith, and F. Hatterman (2005), Effects of parameter uncertainties on the modeling of terrestrial biosphere dynamics, *Global Biogeochem. Cycles*, *19*, GB3020, doi:10.1029/2004GB002395.

1. Introduction

[2] The terrestrial biosphere plays an important role in regulating the increase of atmospheric CO_2 [*Prentice et al.*, 2000]. Process-based models of terrestrial biogeochemical cycles (TBMs) have been successfully used to explain a large proportion of the interannual variation in the CO_2 signal [*Kindermann et al.*, 1996; *Dargaville et al.*, 2002]. TBMs, and dynamic global vegetation models (DGVMs), which further couple terrestrial biogeochemistry to vegetation dynamics, are important tools to investigate the net effect of the complex feedback loops in the global carbon cycle in response to changing environmental forcings such as climate change [*Intergovernmental Panel on Climate Change* (*IPCC*), 2001]. Inter-model comparison studies [*Melillo et al.*, 1995; *Heimann et al.*, 1998; *Cramer et al.*, 1999; *Kicklighter et al.*, 1999; *Cramer et al.*, 2001] and recent applications of TBMs in coupled earth-system models [*Dufresne et al.*, 2002; *Jones et al.*, 2003] have shown that large uncertainty in the response of the global carbon cycle to future climate warming arises as a result of the typical behavior of the particular model used to simulate vegetation changes. Since future projections of atmospheric CO_2 content depend on plausible estimation of the processes governing global carbon exchange, an assessment of the uncertainty associated with these terrestrial ecosystem models is essential to identify key model strengths and deficiencies.

[3] Uncertainty in model simulations can arise from both uncertainty as to the correct (mathematical) description of mechanisms driving ecosystem processes, and from uncertainty in the parameter set to scale mathematical formulations of these processes. Process-based uncertainty can, to some extent, be addressed by inter-model comparison or studies testing different process formulations in one modeling framework [e.g., *Joos et al.*, 2001; *Knorr and Heimann*, 2001; *Smith et al.*, 2001]. Parameter-based uncertainty can result from (1) uncertainty in the measurements used to parameterize a model, (2) the method used to scale, for example, point measurements to the larger

[1]Now at Joint Centre for Hydro-Meteorological Research (JCHMR), Met Office, Wallingford, UK.

0886-6236/05/2004GB002395$12.00

scale on which a model operates, as well as (3) the parameterization of semi-empirical process descriptions, for which parameter values are not readily measurable. Only a few studies have so far analyzed the effects of propagating parameter uncertainty in global vegetation models. Most of these studies have used a local design, i.e., changed one parameter at a time within a given range around the standard value [e.g., *Knorr*, 2000; *Knorr and Heimann*, 2001; *Maayar et al.*, 2002], or used minimum and maximum values from the literature [*Hallgren and Pitman*, 2000]. Although these approaches are able to identify main effects of parameters [*Kleijnen*, 1998], they neglect possible interactions between different parameters, which are important in complex ecosystem models [*Saltelli et al.*, 2000]. Factorial designs [e.g., *White et al.*, 2000a] that allow the assessment of such interactive effects require many model runs and are therefore prohibitive for complex models with a large number of parameters and a high computational demand [*Campolongo et al.*, 2000]. Recently, adjoint methods have been used to infer optimal parameter combinations in terrestrial biosphere models from observations, as well as to gain insight into parameter sensitivities and the uncertainty in output variables [*Wang et al.*, 2001; *Randerson et al.*, 2002; *Rayner et al.*, 2005].

[4] We adopt a Monte Carlo-type stratified sampling approach (Latin hypercube sampling, LHS [*McKay et al.*, 1979]) as an efficient method to identify functionally important parameters and simultaneously estimate the uncertainty range of the modeled results. Like other probability-based methods, LHS allows interactions between different parameter combinations to be studied, and can identify the contributions of parameters alone and in combination to the uncertainty of the modeled results. LHS has previously been used to construct a reduced form of a land surface model for sensitivity tests [*Beringer et al.*, 2002], and has been shown to provide reliable estimates of the distribution function of model output variables [*Helton and Davis*, 2000].

[5] Dynamic global vegetation models are fairly general, globally parameterized models, describing vegetation in terms of plant functional types (PFTs), and its response to variation in climate, atmospheric CO_2 and soil properties [*Steffen et al.*, 1996; *Cramer et al.*, 2001]. They incorporate mechanistic formulations of physiological, biophysical and biogeochemical ecosystem processes (e.g., canopy biophysics, vegetation physiology, phenology, and ecosystem carbon (C) and water (H_2O) cycling) coupled to a description of the major processes governing changes of vegetation structure and composition [*Cramer et al.*, 2001]. Although DGVMs differ in the detail with which particular processes or scales are represented, they tend to follow a similar structure and share a largely common base of process descriptions and parameters, for example, with respect to canopy energy balance, photosynthesis, water balance, respiratory processes, carbon allocation and turnover within the plant, litter and soil organic matter (SOM) decomposition, and plant mortality and establishment [*Woodward et al.*, 1995; *Foley et al.*, 1996; *Friend et al.*, 1997; *Daly et al.*, 2000; *Sitch et al.*, 2003].

[6] In this study, we use the Lund-Potsdam-Jena model (LPJ-DGVM [*Smith et al.*, 2001; *Sitch et al.*, 2003]), which is typical of DGVMs as a family of models, both with respect to its representation of structural ecosystem components (plants and soil) and ecosystem processes. LPJ-DGVM has been used recently to study the sensitivity of equilibrium C storage to climate and atmospheric CO_2 [*Gerber et al.*, 2004] and to assess the uncertainty in simulations of the future terrestrial C balance with respect to both different formulations of ecosystem processes in a DGVM inter-comparison study [*Cramer et al.*, 2001], and different climate change projections from several global circulation models driven with the same radiative forcing [*Schaphoff et al.*, 2005].

[7] The aim of this paper is to systematically analyze the sensitivity of LPJ-DGVM, as a representative DGVM, to its parameterization, and to evaluate the resulting uncertainty in model outcomes both for current and potential future climatic conditions. We examine the relative importance of different parameters for determining specific model results, and analyze the effects of parameter-based uncertainty on modeling terrestrial biosphere dynamics. We also explore possibilities to constrain model uncertainty using independent observations. To facilitate comparison to previously published studies using LPJ-DGVM, we repeat the simulation experiment of the IGBP DGVM Inter-comparison Study [*Cramer et al.*, 2001] using climate data from HadCM2-SUL [*Mitchell et al.*, 1995; *Johns et al.*, 1997] forced by the IS92a emissions scenario [*IPCC*, 1992]. We assume that many of our conclusions in terms of the importance of certain groups of parameters, or their functional equivalents in alternative process formulations, would be similar for DGVMs and similar ecosystem models other than LPJ-DGVM.

2. Methods

2.1. LPJ-DGVM

[8] This study uses the LPJ-DGVM version as described in [*Smith et al.*, 2001; *Sitch et al.*, 2003], with modifications by *Gerten et al.* [2004], and the dark respiration formulation as per *Haxeltine and Prentice* [1996a]. In order to ensure comparability with previous studies using LPJ-DGVM, including *Cramer et al.* [2001], stochastic disaggregation of monthly precipitation to daily values, as implemented by *Gerten et al.* [2004], was not applied in the present study. Instead, precipitation data were, like the other climate variables, interpolated linearly to daily values. Monthly net ecosystem C exchange (*NEE*), which represents the C balance at a point scale, is the difference between heterotrophic respiration (R_h) and net primary production (*NPP*) for each grid cell, i.e.,

$$NEE = R_h - NPP, \tag{1}$$

where negative fluxes denote a net C flux from the atmosphere to the terrestrial biosphere. Annual land-atmosphere flux (also called net biome production, *NBP*, sensu [*Prentice et al.*, 2001]), which represents the landscape scale C balance, is calculated as the sum of the monthly *NEE*s

Table 1. Key LPJ-DGVM Parameters[a]

Parameter	Description
α_a [b]	photosynthesis scaling parameter (leaf to canopy)
α_{C3} [b]	intrinsic quantum efficiency of CO_2 uptake in C3 plants
a_{C3} [b]	leaf respiration as a fraction of Rubisco capacity in C3 plants
α_{C4}	intrinsic quantum efficiency of CO_2 uptake in C4 plants
a_{C4}	leaf respiration as a fraction of Rubisco capacity in C4 plants
a_{leaf}	leaf longevity
α_m	empirical evapotranspiration parameter
CA_{max}	maximum woody PFT crown area
$dens_{wood}$	specific wood density
e_a	respiration temperature response function shape parameter
E_{max} [b]	maximum daily transpiration rate
est_{max} [b]	maximum sapling establishment rate
f_{air} [b]	fraction of the decomposed litter emitted as CO_2 to the atmosphere
f_{inter} [b]	fraction of soil-bound decomposed litter entering the intermediate soil pool
$f_{sapwood}$ [b]	sapwood turnover rate
$fuel_{min}$	minimum fuel load for fire spread
g_m [b]	maximum canopy conductance analogue
g_{min}	minimum canopy conductance
k_{allom1}	crown area = $k_{allom1} \times \text{height}^{k_{rp}}$
k_{allom2}	height = $k_{allom2} \times \text{diameter}^{k_{allom3}}$
k_{allom3}	height = $k_{allom2} \times \text{diameter}^{k_{allom3}}$
k_{beer} [b]	light extinction coefficient
$k_{la:sa}$ [b]	leaf to sapwood area ratio
k_{mort1} [b]	asymptotic maximum mortality rate
k_{mort2}	growth efficiency mortality scalar
k_{rp}	crown area = $k_{allom1} \times \text{height}^{k_{rp}}$
$\lambda_{max,C3}$	optimal c_i/c_a for C3 plants
$\lambda_{max,C4}$	optimal c_i/c_a for C4 plants
$loss_{int}$	interception loss parameter
m_e	litter moisture of extinction
r_{maint} [b]	tissue respiration rate at 10°C
r_{growth} [b]	growth respiration per unit NPP
r_{fire}	fire resistance
τ_{litter} [b]	litter turnover time at 10°C
θ^*	photosynthesis co-limitation shape parameter
z_1	fraction of fine roots in upper soil layer

[a]Detailed information about the parameter range used, and the literature source of this range are given as supplementary material.
[b]These parameters belong to the reduced set of 14 parameters (see section 2.4).

over the year plus annual C lost from biomass burning for each grid cell, i.e.,

$$NBP = NEE + B, \quad (2)$$

where B is biomass burning and negative values indicate storage of C in the terrestrial biosphere, whereas positive values denote release to the atmosphere.

2.2. Parameter Values and Sampling Procedure

[9] Estimates of the ranges of 36 model parameters were, where possible, obtained from an extensive search of the ecological literature to provide a comprehensive overview of the parameter uncertainty (Table 1). For all parameters except leaf longevity the probability distribution function (PDF) was assumed to be uniform. For leaf longevity a triangular distribution was chosen on the basis of data presented by *Reich et al.* [1992]. Following *Sitch et al.* [2003], root turnover time was assumed to be inversely related to leaf longevity. The choice of the parameter-PDF does not influence the ranking of individual parameters in terms of their importance, but could affect the PDF of the modeled output variables. In the case of parameters for which values differ between the different PFTs (i.e., for a_{leaf}, g_{min}, $loss_{int}$, r_{maint}, r_{fire}, and m_e; see Table 1), proportional differences between the different PFT-specific values were conserved when the overall level was adjusted. Latin hypercube sampling [*McKay et al.*, 1979] (see the text file in the auxiliary material[1]) was employed to generate a stratified sample of random sets of parameter values. Unless otherwise stated, parameters were assumed not to be correlated. For 36 (14) parameters under consideration, a sample size of 1000 (400) sets was sufficient to generate, for each model output variable, a reliable estimate of the mean, standard deviation, 90% confidence interval, and ranking of the parameter importance (results not shown).

2.3. Data Sets

[10] Fields of mean temperature, precipitation and cloudiness (1901–2000) were taken from the CRU2000 monthly climate data set on a 0.5° × 0.5° global grid, provided by the Climate Research Unit (CRU), University of East Anglia [*Mitchell et al.*, 2004]. Data on the annual CO_2 content of the atmosphere were obtained from C. D. Keeling and T. P. Whorf, http://cdiac.esd.ornl.gov/trends/

[1]Auxiliary material is available at ftp://ftp.agu.org/apend/gb/2004GB002395.

Table 2. Overview of the Experimental Setup Used in This Study, as Described in Section 2.4

Section	Number of Parameters	Number of LHS Samples	Spatial Resolution	Output Variable	Comments
3.1	36	1000	81 grid cells	(R)PCC for several model output variables	
3.2	14	400[a,b,c]	global 3.25° × 2.5° grid HadCM2-SUL	*A*, *NPP*, vegetation C	
3.3.1	14	400[c]	81 EMDI class A sites	*NPP*	
3.3.2	14	400[c]	6 EUROFLUX sites	*NEE*	simulation without fire
3.3.2	14	400[c]	global 3.0° × 3.0 ° grid CRU2000	seasonal cycle of atmospheric $[CO_2]$	atmospheric transport with TM2
3.3.3	14	400[c]	global 3.25° × 2.5° grid	*NBP*, ecosystem C pools,	
3.3.4			HadCM2-SUL	vegetation structure	

[a]These are 400 LHS samples for 14 completely uncorrelated parameters.
[b]These are 400 LHS samples as above, but with correlation between α_{C3} and α_a (R^2: 80), as well as α_{C3} and k_{beer} (R^2: 70).
[c]These are 400 LHS samples as in the second footnote, used for the calculation of RPCCs; however, for all figures, and output variable ranges, only those of the 400 runs were used that conformed to the benchmarks in section 3.2.

co2/sio-mlo.htm, 2003, last update: June 2004). Time series of monthly temperature, precipitation and *PAR* were obtained for six sites of the EUROFLUX network, i.e., those for which more than 3 years' measurements were available [*Valentini et al.*, 2000]. Soil texture data were based on the FAO soil data set [*Zobler*, 1986; *Food and Agriculture Organizaton*, 1991; *Haxeltine and Prentice*, 1996a]. The response of the terrestrial biosphere to climate change was simulated using monthly climate data (1861–2100) on a 3.75° × 2.5° grid, derived from HadCM2-SUL [*Mitchell et al.*, 1995; *Johns et al.*, 1997] forced by CO_2 concentrations corresponding to the IPCC IS92a scenario [*IPCC*, 1992], as used by *Cramer et al.* [2001].

[11] An assessment of the uncertainty in model results requires some understanding of the typical variation of the considered variables in reality. Spatially referenced data useable for the evaluation of global vegetation models are still very sparse [*Cramer et al.*, 1999; *Scurlock et al.*, 1999]. We evaluated model performance against *NPP* data from the Ecosystem Model Data Inter-comparison project (EMDI) for 81 sites from the class A data set (R. J. Olson et al., http://www.daac.ornl.gov, 2001, last update: June 2004) that include measurements for all major biomes. Seasonality of net C fluxes was compared to (1) point-scale measurements of *NEE* obtained with eddy-covariance techniques at six sites of the EUROFLUX network [*Valentini et al.*, 2000], and (2) the seasonal cycle of CO_2 observed at 27 monitoring stations from a program of the National Oceanographic and Atmospheric Administration [*GLOBALVIEW-CO_2*, 1999].

2.4. Modeling Protocol

[12] For each LHS set the model was run for a "spin-up" period of 900 years, to achieve equilibrium in terms of pre-industrial stable vegetation structure and C pools. During the spin-up phase, 30 years of varying climate from the beginning of the respective climate data set were repeated continuously with pre-industrial atmospheric CO_2 content. The model was thereafter driven with the transient climatology and observed atmospheric CO_2 content. Table 2 summarizes the experimental setup of this study.

[13] Running LPJ-DGVM several hundred times for the entire globe at 0.5° resolution is computationally not feasible. In order to assess the parameter-based uncertainty on the global scale, we attempted to identify the most important parameters contributing to overall model uncertainty, and performed a global-scale uncertainty analysis with this reduced set. Parameter importance for all 36 parameters was determined at a set of locations spanning all major biomes, and corresponding to EMDI class A sites. 30-year average values (1961–1990) of each model output variable were used to analyze the parameter importance (section 3.1). Fourteen parameters could be identified as having the greatest influence on the ecosystem carbon cycling (section 3.2; absolute ranked partial correlation coefficient, RPCC > 0.25; see auxiliary material for definition), as well as being of substantial importance in modeling vegetation dynamics and terrestrial water balance. We chose $|RPCC| = 0.25$ as a lower threshold for parameter importance because visual inspection of correlation plots between parameter and model output did not show any notable trend for RPCCs below this value. By using this reduced set of 14 parameters, we could reduce the numbers of required runs to a practically attainable level of 400, while still accounting for most of the model uncertainty.

[14] CRU2000 monthly climate data were used to estimate 30-year average *NPP* (1961–1990) for 81 EMDI cells (section 3.3.1). Site-specific regressions between measured meteorology and the nearest grid cell from the CRU climatology for each of the six EUROFLUX sites were used for the spin-up and in the transient run-up to the period for which site-specific meteorological data were available; site-specific data were used where possible (section 3.3.2). For consistency in the comparison to eddy covariance measurements, fire disturbance was not included in the simulations performed for this comparison. Site history may influence the magnitude and sign of the annual C exchange [*Thornton et al.*, 2002], but, consistent with recent findings from flux measurements [*Kolari et al.*, 2004], we did not find any notable effect on the modeled seasonal cycle (Stephen Sitch, unpublished results, 2003). Global fields of averaged and detrended monthly *NBP* for the period 1983–1992 were obtained using CRU2000 monthly climatology aggregated to 3.0° × 3.0° resolution (section 3.3.2). This was the highest resolution possible given the computational constraints associated with performing 400 global simulations. These data were passed into a reduced-form version of the atmospheric transport

Table 3. The Twelve Most Important Parameters in Controlling C Fluxes and Pools[a]

	NPP		R_h		VegC		Litter C		Intermediate Soil C		Slow Soil C	
Rank	Parameter	RPCC	Parameter	RPCC	Parameter	RPCC	Parameter	RPCC	Parameter	RPCC	Parameter	RPCC
1	α_{C3}	0.846	α_{C3}	0.801	α_{C3}	0.607	α_{C3}	0.791	f_{air}	−0.837	f_{inter}	−0.873
2	α_a	0.704	α_a	0.662	$f_{sapwood}$	0.536	τ_{litter}	0.742	α_{C3}	0.783	f_{air}	−0.720
3	θ	0.474	g_m	0.467	k_{mort1}	−0.459	α_a	0.593	α_a	0.619	α_{C3}	0.657
4	g_m	0.463	θ	0.429	$k_{la:sa}$	−0.398	θ	0.405	θ	0.392	α_a	0.473
5	r_{growth}	−0.297	k_{beer}	−0.303	g_m	0.379	g_m	0.397	g_m	0.298	θ	0.289
6	k_{beer}	−0.270	r_{growth}	−0.255	α_a	0.370	$f_{sapwood}$	0.321	k_{beer}	−0.244	g_m	0.270
7	a_{C3}	−0.268	a_{C3}	−0.242	est_{max}	−0.318	r_{growth}	−0.252	r_{growth}	−0.205	k_{beer}	−0.188
8	$f_{sapwood}$	0.230	a_{leaf}	0.201	θ	0.257	a_{C3}	−0.224	a_{C3}	−0.200	a_{C3}	−0.153
9	a_{leaf}	−0.217	$f_{sapwood}$	−0.192	k_{mort2}	0.186	a_{leaf}	−0.193	a_{leaf}	−0.177	r_{growth}	−0.149
10	r_{maint}	−0.134	α_m	0.112	k_{allom2}	0.171	E_{max}	0.149	f_{inter}	0.160	$\lambda_{max,C3}$	0.133
11	$\lambda_{max,C3}$	0.132	r_{maint}	−0.110	z_1	−0.149	k_{beer}	−0.146	$\lambda_{max,C3}$	0.159	E_{max}	0.123
12	E_{max}	−0.128	$\lambda_{max,C3}$	−0.109	a_{C3}	−0.143	r_{maint}	−0.121	E_{max}	0.140	a_{leaf}	−0.106

[a]Further results are given in the auxiliary material. Given here are net primary production (*NPP*), heterotrophic respiration (R_h) as well as vegetation, litter and soil C pools (soil C partitioned into pools with intermediate and slow turnover times). The ranking was performed according to the average RPCC across all 81 grid cells. Regionally, the importance ranking may vary, as discussed in the text. Parameters specific to C4 plants have similar importance than the respective parameters for C3 plants locally; however, they are or minor importance globally because of the limited geographical distribution of C4 plants.

model TM2 [*Heimann et al.*, 1998; *Kaminski et al.*, 1999a, 1999b]. Modeled seasonal cycles were compared against the global network of atmospheric CO_2 monitoring sites, following the approach of *Heimann et al.* [1998]. Global C cycle simulations for 1861–2100 were performed with the HadCM2-SUL climate data at 3.75° × 2.5° resolution [*Cramer et al.*, 2001, sections 3.3.3 and 3.3.4]. No notable differences in terms of global net assimilation rate, *A* (gross primary production, *GPP*, minus leaf respiration, R_l), *NPP* and ecosystem C pools were observed between simulations using climatologies at 0.5° and 3.0° or climate model resolution under the standard parameterization. Also the seasonal cycle of CO_2 at all 27 stations was very similar between simulations using climatologies at 0.5° and 3.0° resolution.

2.5. Parameter Constraints and Global Benchmarking

[15] The parameters scaling various ecosystem processes are likely to be interdependent to a greater or lesser extent, for example because of the existence of syndromes of structural and functional characteristics, such as plant life history strategies. In our analyses, we varied parameters within their literature range without assuming any interdependence. This might cause overestimation of uncertainty, and thereby unjustifiably reduce confidence in model results [*Helton and Davis*, 2000]. Inverse methods have been recommended as an approach to constrain model uncertainty and to infer parameter correlations [*Kaminski et al.*, 2002; *Rayner et al.*, 2005]. However, such methods are beyond the scope of this paper.

[16] To limit the overestimation of uncertainty due to parameter interdependence, a simpler approach, taking advantage of existing knowledge of the terrestrial biosphere, is to evaluate model performance against generally agreed benchmarks of the contemporary carbon cycle. If the model in its standard parameterization produces output that conforms to the benchmarks, the failure to meet the benchmarks in a particular run may be the consequence of unrealistic or implausible combinations of particular parameters, even if each individual parameter range may be justified on the basis of literature values. Correlations between these parameters can then be prescribed to avoid these combinations, while still sampling parameter values uniformly across each parameter range [*Iman and Conover*, 1982].

[17] In our study, we identified one such set of parameters (section 3.2). Expert judgment would have allowed further exclusion of parameter combinations that produce unrealistic results for particular geographical regions or biomes. In the interest of objectivity, however, we employed the same parameter space globally. In sections 3.3 and 3.4, to evaluate the uncertainty of other model outcomes, in particular under climate change scenarios, we choose to consider only those runs, which satisfy generally agreed global benchmarks of both global production and vegetation C. Net assimilation rate *A* in the range of 90–160 PgC yr^{-1}, *NPP* in the range of 45–85 PgC yr^{-1} and vegetation C in the range of 500–1200 PgC were taken as parameter constraints. The benchmarks were based on top-down studies of the global C cycle [*Knorr and Heimann*, 1995; *Ciais et al.*, 1997] and estimates of various process-based models of potential natural vegetation [*Houghton and Skole*, 1990; *Post et al.*, 1997; *Cramer et al.*, 1999; *Gerber et al.*, 2004]. A similar approach has been applied in a comparable study on climate model uncertainty [*Knutti et al.*, 2002].

3. Results

3.1. Parameter Importance

[18] The most important parameters controlling *NPP* are the intrinsic quantum efficiency for C3 plants α_{C3} (RPCC = 0.85), which influences the amount of energy available for *GPP*, and the parameter α_a (RPCC = 0.70), which primarily accounts for photosynthetically active radiation (*PAR*) absorbed by non-photosynthetic structures (e.g., branches) and thus lost to canopy photosynthesis (Table 3). Of secondary importance are the shape parameter θ (RPCC = 0.47), controlling the degree of co-limitation by light and Rubisco activity in the Farquhar photosynthesis scheme [*Haxeltine and Prentice*, 1996b], and the canopy light extinction coefficient, k_{beer} (RPCC = −0.27), which determines the shape of the relationship between canopy leaf area index (*LAI*) and the fraction of incoming *PAR* absorbed

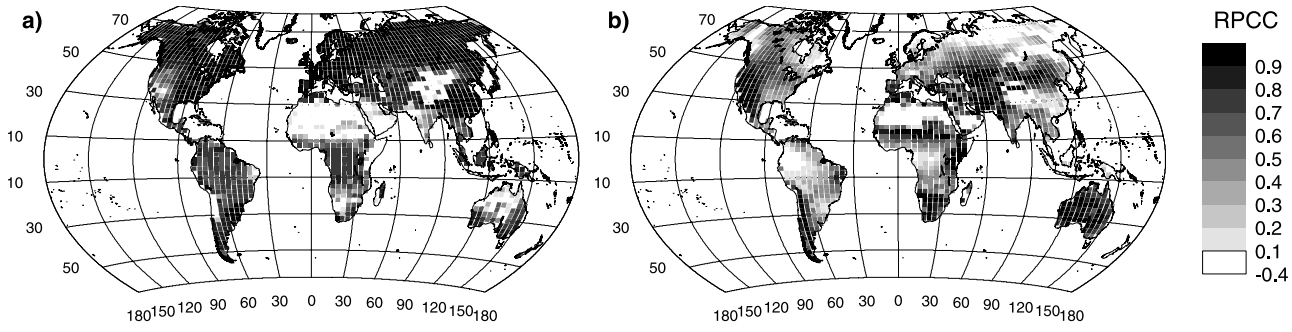

Figure 1. Parameter importance, measured as RPCC, of (a) α_{C3} and (b) g_m for *NPP* from global simulations, using 14 parameters and 400 LHS samples.

by the canopy. Parameters governing autotrophic respiration (R_a) have also notable, though less pronounced, effects on annual *NPP*, with higher respiration rates reducing *NPP* (RPCC = −0.29, −0.27, −0.13, for r_{growth}, a_{c3}, r_{maint}, respectively).

[19] Although these parameters have a similar effect on *A* and *NPP* worldwide, differences in parameter importance can be observed in water-limited regions as characterized by a low ratio of actual to potential evapotranspiration. In such regions, parameters controlling plant water balance, i.e., g_m (RPCC = 0.46), E_{max} (RPCC = 0.13) and α_m (RPCC = −0.11) are relatively important (Figure 1). E_{max} controls the water extraction supply, whereas g_m and α_m describe the coupling of the atmospheric water demand to the leaves. Assuming constant non-water stressed stomatal conductance, higher α_m increases the demand, whereas higher values of the canopy conductance analogue g_m reduces it. Together these parameters scale stomatal regulation and C uptake. Since stomata couple the C and H_2O cycles, the same parameters also control actual evapotranspiration and freshwater recharge (see auxiliary material, Table S2). Other parameters influential in regulating the water balance are those determining photosynthetic activity, LAI, and the stomatal conductance associated with a certain assimilation rate, which in turn depends on the choice of the optimal ratio of intercellular to ambient CO_2 partial pressure, $\lambda_{max,C3}$.

[20] *NPP* determines the amount of C available for tissue production and thereby controls C storage in vegetation (Table 3). The rate of conversion of sapwood to heartwood, $f_{sapwood}$ (RPCC = 0.54), and the leaf-to-sapwood-area ratio, $k_{la:sa}$ (RPCC = −0.40), control C residence times in trees, and therefore the size of the vegetation C pool. Larger $f_{sapwood}$ values result in trees with proportionally less sapwood, smaller associated losses to R_a, and proportionally more heartwood, and thus generally larger C stocks and a higher C accumulation rate after disturbance. Larger values for $k_{la:sa}$ decrease the amount of C required for leaves and their associated transport tissue (''pipe-model''), and thereby enhance *LAI* (RPCC = 0.60), light interception and *NPP*. At the same time, increased C storage in leaves in connection with larger $k_{la:sa}$ values lead to reduced C accumulation as wood. Vegetation dynamics processes are the third major control on vegetation C. Higher disturbance rates (higher maximum mortality k_{mort1}; RPCC = −0.46) and higher establishment rates est_{max} (RPCC = −0.32) lead to younger average vegetation, with less C stored.

[21] Soil C stocks are controlled by f_{inter} and f_{slow} (RPCC = −0.81, −0.80), which together determine the mean residual time of C as SOM. Parameters governing litter fall are almost as important (α_{C3} RPCC = 0.75, α_a RPCC = 0.58). Notably, uncertainty in τ_{litter} has very little influence on overall SOM stock, as litter C very quickly comes to equilibrium with annual litter fall, and the size of the litter pool, though controlled by τ_{litter}, is small compared to overall soil C stocks.

[22] Fire frequency is influenced by parameters regulating fuel load (vegetation and litter C), and fire susceptibility, for example the moisture threshold for fire extinction (m_e: RPCC = 0.48). Dryness of the litter layer, a third important factor, depends on parameters governing the root water uptake (z_1: RPCC = 0.43; E_{max}: RPCC = 0.35), and plant water use (g_m: RPCC = −0.34), as in the model soil moisture in the top layer is taken as a surrogate for litter moisture. The C flux from biomass burning depends very strongly on the vegetation C pool ($f_{sapwood}$: RPCC = 0.41; k_{mort1}: PRCC = −0.38).

[23] Since LPJ-DGVM is spun up to equilibrium in terms of its pre-industrial C pools, the annual C release from R_h and biomass burning must balance annual C inputs from *NPP*, averaged over the final few years of the spin-up. The size of the different C pools, their average turnover time and their C inputs are then in balance. Despite large uncertainty in vegetation and soil C pools, R_h is thus strongly controlled by parameters regulating *NPP*. With increased productivity an ecosystem exhibits a larger seasonal amplitude of *NEE*, as a consequence of greater C uptake in summer, and greater C release in winter associated with larger ecosystem C stocks, in effect amplifying the differential responses of *NPP* and R_h to seasonal variations in climate. Most of the remaining uncertainty in the seasonal cycle of *NEE* is associated with the sensitivity of photosynthesis to water stress (see auxiliary Figure S2). A set of model parameters that describes high non-water-stressed stomatal conductance (a result of high potential daily *GPP*), with a well-coupled canopy-atmosphere system (high α_m and low g_m), and low water uptake rates (low E_{max}), increases the sensitivity of actual stomatal conductance, and thus actual *GPP*, to plant water stress. Particularly in water-limited environments and/or dry conditions, this higher sensitivity increases the effect of summer drought on stomatal conductance, and thus reduces *NPP*. R_h is less sensitive to seasonal variations in soil moisture, owing to its direct dependence on

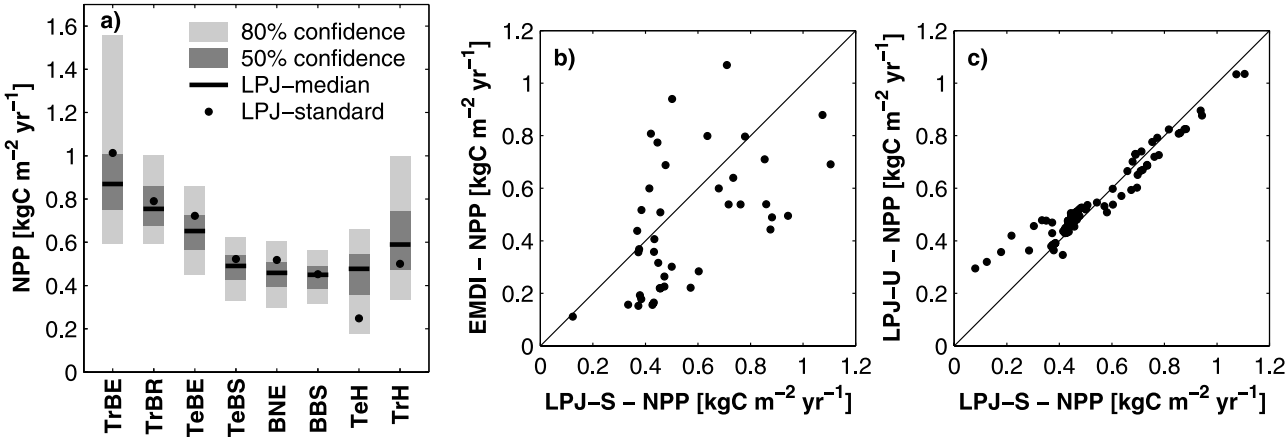

Figure 2. (a) Average annual *NPP* (kgC m^{-2} yr^{-1}) for various biomes for 1961–1990, and its parameter-based uncertainty range. Correlation of annual NPP between (b) LPJ-DGVM (standard parameterization, LPJ-S) and EMDI *NPP*-data (EMDI), for sites at which the modeled and observed vegetation type are in agreement; and (c) between LPJ-DGVM under standard parameterization (LPJ-S) and the median of the uncertainty experiment (LPJ-U). Nomenclature of the plant functional types (PFTs): TrBE, tropical broadleaved evergreen; TrBR, tropical broadleaved rain green; TeNE, temperate needle-leaved evergreen; TeBS, temperate broadleaved summer green; BNE, boreal needle-leaved evergreen; BNS, boreal needle-leaved summer green; BBS, boreal broadleaved summer green; TeH, temperate herbaceous; TrH, tropical herbaceous.

the size of the litter and soil C pools, which varies comparatively little between seasons. Thereby uncertainty in *NPP* is the main source of uncertainty in magnitude and interannual variations of modeled *NEE*.

[24] Most of the variation in vegetation composition, expressed as foliar projective cover (FPC) of individual PFTs, can be explained by (1) factors that control the competitive balance between dominant and subdominant PFTs for a given climate and pedographic setting; and (2) factors influencing the competitive strength of a specific plant functional trait. Generally, parameters determining ecosystem level productivity and key vegetation dynamic parameters appear to have the greatest influence on the vegetation structure. Water balance and stand structure related parameters are of lesser importance, except under arid conditions in which savanna type ecosystems prevail. This is a result of changes in the delicate balance between water demand and supply. In general, forest ecosystems are favored by higher maximum soil water extraction rates, E_{max}, and higher g_m, since a less coupled canopy-atmosphere system mitigates the effect of high atmospheric water demand on plant transpiration.

[25] Parameter combinations describing stable vegetation dynamics (lower maximum mortality, stronger effect of growth efficiency on mortality, and higher re-establishment rate) tend to increase the FPC of the dominating PFT. A faster rate of canopy closure, resulting from higher k_{allom1}, k_{allom3}, and a lower self-thinning coefficient k_{rp} also favor the dominant PFT, with the strongest effect on the herbaceous understorey. The predominant influence on the FPC of herbaceous PFTs is exerted by the canopy light extinction coefficient, k_{beer}, with reduced *PAR* within the canopy increasing the available radiation at the forest floor and tipping the competitive balance toward the herbaceous PFTs. The response of FPC to k_{beer} is highly non-linear (PRCC = −0.81; PCC = −0.41), as the canopy light extinction, and thus *PAR* utilization, follow the Lambert-Beer law.

3.2. Constraints to the Parameter Space

[26] Of the 36 parameters in Table 1, 14 parameters can be identified as having a dominant influence on the terrestrial carbon cycling (|RPCC| > 0.25; marked in Table 1 with an asterisk). Global simulations using the reduced set of parameters result in an uncertainty range in global *NPP*, for one model, of 29.8 to 133.3 PgC yr^{-1}, spanning the complete range of *NPP* estimates reported from an earlier model intercomparison (44.4–66.3 PgC yr^{-1} [*Cramer et al.*, 1999], and exceeding the variable constraints set in section 2.5. Uncertainty in global *A* and *NPP* mainly results from uncertainty in α_{C3}, α_a, and k_{beer}, and in particular from the consequences of extreme combinations of these parameters for light-use efficiency (see auxiliary Figure S1). By prescribing correlations between these parameters, while still sampling parameter values uniformly across the total parameter range, as described in section 2.5, implausible combinations are avoided, and uncertainty in modeled *NPP* is substantially reduced (43.1–103.3 PgC yr^{-1}). Similar reductions are achieved for *A* (without parameter correlation: 51.5–224.1, with parameter correlation: 71.9–172.6 PgC yr^{-1}).

[27] The set of parameter combinations is further reduced by excluding runs in subsequent analyses that do not conform to global benchmarks on the contemporary carbon cycle (see section 2.5). 73% of the 400 simulations satisfy the global constraints for *A* or *NPP*, whereas only 41% fulfill the constraint on vegetation C. Only 28% out of the 400 runs satisfy the benchmarks for both global production

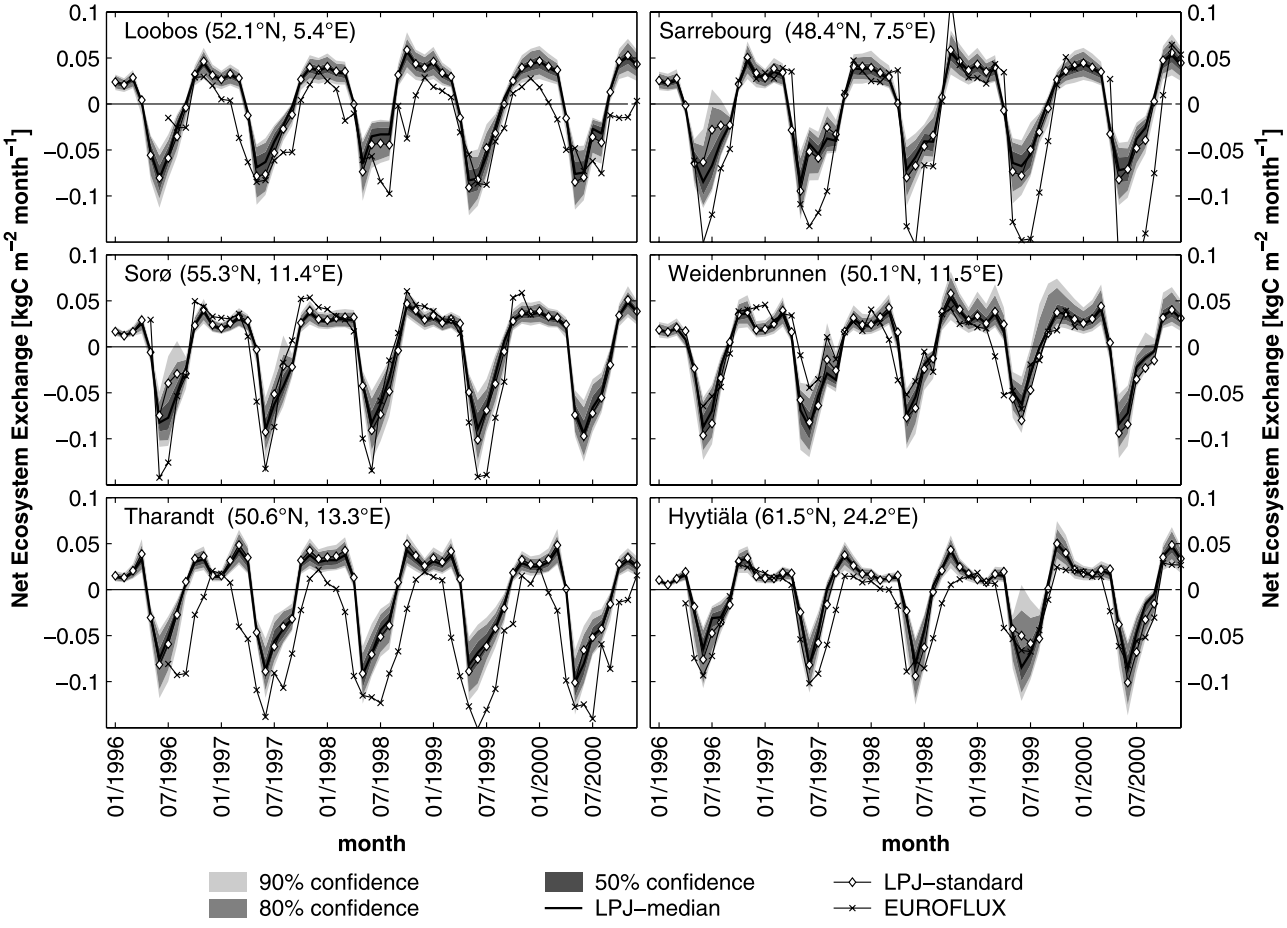

Figure 3. Simulated and observed net ecosystem exchange (*NEE*, kgC m^{-2} $month^{-1}$) for 1996–2000 at six eddy-covariance sites of the EUROFLUX network. Data are taken from *Valentini et al.* [2000]. Statistics are available in auxiliary Table 4. See color version of this figure at back of this issue.

and vegetation C. Most of the runs excluded have extreme parameter combinations of either α_{C3} versus g_m or $f_{sapwood}$ and k_{mort1} versus $k_{la:sa}$. The first case is associated with low quantum efficiency combined with high water stress, leading to low C uptake. The second is tied to unrealistic vegetation dynamics in regions with stable growing conditions for forests (e.g., Amazonia and tropical Africa) for very low $k_{la:sa}$ in combination with low k_{mort1} and high $f_{sapwood}$.

3.3. Parameter-Based Uncertainty in Modeling the Present-Day Carbon Cycle

3.3.1. Local Scale Annual Net Primary Production

[28] *NPP* estimates of LPJ-DGVM are in rather modest agreement with the *NPP* data from the EMDI data set (Figure 2b). However, the fit is comparable to the fit observed with other terrestrial ecosystem models (EMDI, unpublished data, 2003, http://gaim.unh.edu/Structure/Intercomparison/EMDI/). In principle, parameter-based uncertainty suffices to explain the difference observed between modeled and measured *NPP* for most sites (Figure 2a). The results of running LPJ-DGVM with its standard parameterization agree very well with the median of the uncertainty experiment (Figure 2c). Sources of disagreement between model and data, apart from parameter-based model uncertainty, include the intrinsic difference between site measurements and values applicable at larger (e.g., regional, biome, global) scales, taking account of variation in climate, pedography, topography, land management etc. at intermediate scales. In addition, uncertainty arises from the measurements themselves, in particular from the assumptions made to estimate below-ground C allocation [*Clark et al.*, 2001]. Previously, the utility of field measurements to evaluate the performance of TBMs has been questioned on the basis of the observation that, as in this study, the *NPP* data set did not show any particular sensitivity to annual precipitation [*Knorr and Heimann*, 2001]. The explanation for this may lie in differences in the period of *NPP* sampling and climate measurements.

3.3.2. Seasonal Cycle of Net Ecosystem Exchange

[29] Simulated *NEE* of the median of the sensitivity experiment and the standard parameterization agree reasonably well with the seasonal phasing and amplitude observed at the six eddy covariance sites considered (Figure 3). Generally, the seasonal cycle is well captured by all simulations of the uncertainty experiment, compared to the standard run. The uncertainty range of *NEE* is considerably smaller than the uncertainty range of modeled *NPP*. For

Table 4. Normalized Mean Standard Deviation (NMSD) Between Measured and Modeled Mean Seasonal Cycle of CO_2 at 27 Stations From the GLOBALVIEW Network, Pooled Into Northern Stations (12), Tropical Stations (9) and Southern Stations (6), and Parameter Importance Determining NMSD, Measured as Average RPCC Over All Stations Within a Specific Group[a]

	All Stations	Northern Stations (>25°N)	Tropical Stations (25°N–30°S)	Southern Stations (>30°S)
		NMSD		
Median	13.1	17.6	10.0	7.6
Min	1.5	5.0	1.2	1.1
Max	38.8	35.9	40.6	39.7
		RPCC		
g_m	0.78	−0.02	0.78	0.89
α_{C3}	−0.50	−0.63	−0.63	0.53
τ_{litter}	−0.44	−0.34	−0.42	−0.34
α_a	−0.36	−0.48	−0.55	0.35
Θ	−0.30	−0.50	−0.36	0.45
r_{growth}	0.23	0.44	0.31	−0.37

[a]See also the auxiliary material.

Sorø and Sarrebourg the simulations agree well on the seasonality; however, peak C uptake in summer is consistently underestimated by the simulations. Simulated net C uptake is consistently too low in Tharandt, whereas the seasonality matches the measurements reasonably well.

[30] The root mean square error (RMSE, see auxiliary material) between the flux measurements and simulations is most influenced by α_{C3}, α_a and r_{growth} for Loobos, Sarrebourg, Sorø and Bayreuth, since these govern the amplitude of the seasonal cycle. However, the effect is the opposite for Sarrebourg/Sorø, where LPJ-DGVM underestimates the seasonal cycle, compared with Bayreuth/Loobos, where peak C uptake is well matched. Variation of g_m can, as noted earlier, lead to considerable uncertainty in monthly *NEE*. The effect of parameters on the modeled error varies between the measurements sites, both in terms of their average importance and ranking, as well as the seasonal cycle of parameter importance.

[31] LPJ-DGVM is capable of simulating the dominant features of the seasonal cycle of CO_2 as measured at the global network of atmospheric CO_2 monitoring stations. The normalized mean square deviation (NMSD, see supplement) between model and measurements considering all 27 stations is only slightly larger than the deviation observed with six TBMs, including a previous model, BIOME-2, related to LPJ-DGVM [*Heimann et al.*, 1998]. The range of NMSD obtained from the uncertainty experiment is of similar magnitude when pooled into three latitudinal categories (Table 4). The strong influence of the terrestrial biosphere on the seasonal cycle at northern high-latitude stations is reflected in a relative high uncertainty in the modeled seasonal cycle of CO_2. The consistent too early draw down and recovery of CO_2 for these stations, which was already apparent in a predecessor model to LPJ-DGVM, BIOME-2 [*Heimann et al.*, 1998], cannot be related to uncertainty in the parameters examined, and thus appears to be a robust model feature. Likely causes are the effect of snow cover on soil thermodynamics and hence rates of R_h [*McGuire et al.*, 2000], and the delayed onset of the growing season associated with snow cover and frozen soils.

[32] Parameters governing plant C uptake generally play an important role (α_{C3}: RPCC = −0.50; α_a: RPCC = −0.36) in determining NMSD. In particular, higher values for α_{C3} and α_a increase the agreement between model and observations at the northernmost stations, mainly because of increased summer draw down of CO_2 concentrations by ecosystems. Of the parameters controlling vegetation and SOM dynamics, only τ_{litter} appears to be important globally (RPCC = −0.43), with increasing litter residence time amplifying the seasonal cycle at all stations. A marked reduction in global average NMSD is apparent for low values of g_m (RPCC = 0.77). However, this reduction is mainly associated with tropical and southern stations, which have a low amplitude and little modeled uncertainty in the seasonal cycle of CO_2, so that the reduced absolute model error is rather small. Notably, no significant relationship exists between the overall model performance with respect to the CO_2 network and predicted biosphere properties such as global *A* and *NPP*.

3.3.3. Contemporary Terrestrial Biosphere Dynamics

[33] Variation of present-day vegetation composition due to parameter-based uncertainty is typically within ±12.5% of the median FPC (90% confidence interval) for tropical and temperate tree PFTs, with a larger range for boreal (±15%) and particularly herbaceous PFTs (±21.5%). Global vegetation maps of the distribution of evergreen, deciduous, and mixed forests, grasslands and deserts show good agreement (average κ = 0.74 [*Prentice et al.*, 1992]) with the median vegetation composition. Global *A* and *NPP* under the standard parameterization and the respective median estimates from the uncertainty experiment are within 10% of the most plausible estimates of global *A* and *NPP* from observations (Table 5). Estimates of C lost from biomass burning are of a similar magnitude to the 4.3 PgC yr^{-1} (±50%) estimated from observations by *Andreae and Merlet* [2001]. Mean annual land-atmosphere fluxes for the 1980s and 1990s are estimated at −1.48 (−0.37 to −2.43) and −1.71 (−0.37 to −3.25) PgC yr^{-1}, respectively.

[34] Figure 4 shows the spread in land-atmosphere flux estimates with and without the constraints discussed in section 2.5. Median estimates of annual *NBP* are within ±0.1 PgC yr^{-1} for the period in 1981–2000; the unconstrained median is in the direction of a stronger C uptake. The larger spread without the constraints results mainly from parameter combinations affecting present-day *A* and *NPP*, whereas vegetation C contributes only little

Table 5. Standard Results, Median and 90% Confidence Range of the Uncertainty Experiment for Present-Day Global C Fluxes (PgC yr^{-1}), Terrestrial C Storage (PgC) and H_2O Fluxes (10^{12} m^3 yr^{-1})

	1980s		1990s	
	Standard	Median (90% Confidence)	Standard	Median (90% Confidence)
A	111.6	109.0 (89.9–143.7)	114.8	112.5 (92.8–148.8)
NPP	61.9	60.8 (48.9–78.1)	63.3	62.7 (50.5–80.1)
Rh	55.1	54.3 (42.8–70.6)	56.7	56.0 (44.9–72.5)
Biomass burning	5.5	5.1 (3.0–7.5)	5.4	5.1 (3.0–7.4)
Land-atmosphere flux	−1.5	−1.5 (−0.4–−2.4)	−1.7	−1.7 (−0.4–−3.2)
Vegetation C	995	902 (556–1151)	1004	912 (566–1157)
SOM	1441	2323 (877–5181)	1450	2329 (884–5191)
Annual AET	37.9	34.1 (26.2–45.0)	37.4	33.8 (26.0–44.7)
Annual runoff	36.0	45.0 (34.7–55.1)	35.6	44.6 (34.2–54.5)

to the uncertainty in present-day *NBP*, except for some outliers. The response of *A* and *NPP* to observed climate and CO_2 changes relative to present-day *A* and *NPP* is comparable between all runs. This means that, in absolute terms, the response is amplified by larger values of *A* and *NPP*. As a consequence, 68% and 54% of the variance in the increase in magnitude of *NBP* are explained by present-day *A* and *NPP*, respectively, using linear regression without the constraints. Uncertainty in global *A* accounts for only 22% of the uncertainty in the contemporary C uptake for the constrained case.

3.4. Model Projections to 2100

[35] The increases in *A* and *NPP* under the climate change scenario from HadCM2-SUL, forced with the IS92a emissions scenario, are a robust model feature, and are driven by the continuous increase in atmospheric CO_2 as well as CO_2 induced increases in water-use efficiency. Despite the uncertainty in *A*, *NPP*, vegetation distribution and modeled water stress (allowed for by varying the parameter g_m over a wide range), projected changes in water-use efficiency are robust model results in the sense that alternative parameter values do not change the direction of this important process response (see auxiliary Figure S5). As a result of the rise in *A*, global land-atmosphere fluxes increase in magnitude by the 2050s to −4.85 (−3.34 to −6.58) PgC yr^{-1}, but then decrease to −3.36 (−1.84 to −4.80) PgC yr^{-1} by the end of the twenty-first century (Figure 5a). This decline is a consequence of the leveling off of C uptake in vegetation and the decline in soil C uptake with land-atmosphere fluxes of around −2.51 (−1.63 to −3.38) PgC yr^{-1} (Figure 5b) and −0.75 (−0.01 to −1.88) PgC yr^{-1} (Figure 5c), respectively, toward the end of the twenty-first century. These trends are relatively robust on a long timescale (50 years; average R^2 with linear regression: 0.98), and in reasonable agreement with previously published LPJ-DGVM results [*Cramer et al.*, 2001]. Most of the deviation among the suite of runs in this study occurs in the last 2 decades of the twenty-first century, when some simulations show a stagnation of the biospheric C uptake, whereas others exhibit a strong decrease, mainly as result of C losses from soil. Decadal and inter-annual variations are less well constrained (average R^2 = 0.88/0.86 for decadal and inter-annual variability, respectively), but still reasonably similar to the median of the uncertainty experiment.

[36] Parameters governing present-day plant C uptake (α_{C3}, α_a, θ) exert some influence on the rate of increase in *A* and *NPP*, but have only little impact on the rate of vegetation C build-up, which are much more strongly controlled by vegetation dynamics (k_{mort1} and k_{est}, 0.67% explained variance; stepwise ANalysis Of VAriance (ANOVA)). Global SOM C uptake at the end of the twenty-first century, by contrast, is influenced to a similar extent by parameters controlling present-day *NPP* (α_{C3}, α_a, θ r_{growth}) and parameters governing vegetation and SOM dynamics (f_{inter}, τ_{litter}, k_{est}, 0.45% and 0.40% explained variance respectively, stepwise ANOVA).

[37] Projected *NBP* at the end of the twenty-first century shows distinct regional patterns, however, the changes compared to present-day *NBP* are not as robust as modeled changes in *A* and *NPP*. The latitudinal breakdown of the development of the land-atmosphere flux over the twenty-first century shows that the rise in atmospheric CO_2 increases C storage in both the tropics and the northern extra tropics up to 2050 (see auxiliary Figure S4). Thereafter climate change substantially weakens the capacity of ecosystems to sequester C in the tropics and southern midlatitudes by the end of the twenty-first century, in

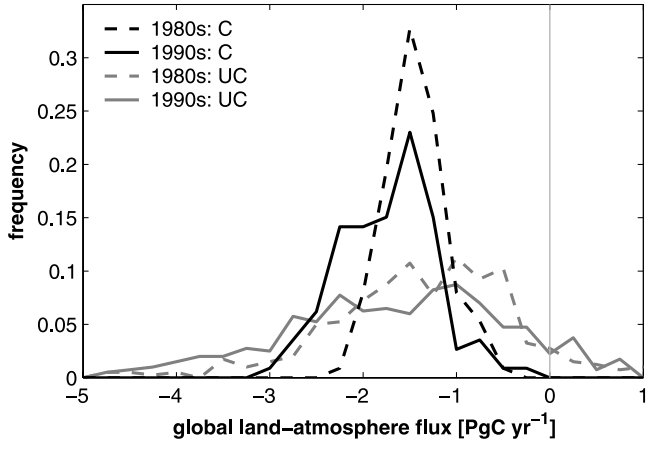

Figure 4. Global land-atmosphere flux (PgC yr^{-1}) in the 1980s and 1990s, resulting from observed climate and atmospheric CO_2 changes. "UC" denotes the full uncertainty range, whereas "C" refers to the uncertainty range for those model realizations that conform to contemporary observations of *A*, *NPP* and vegetation C.

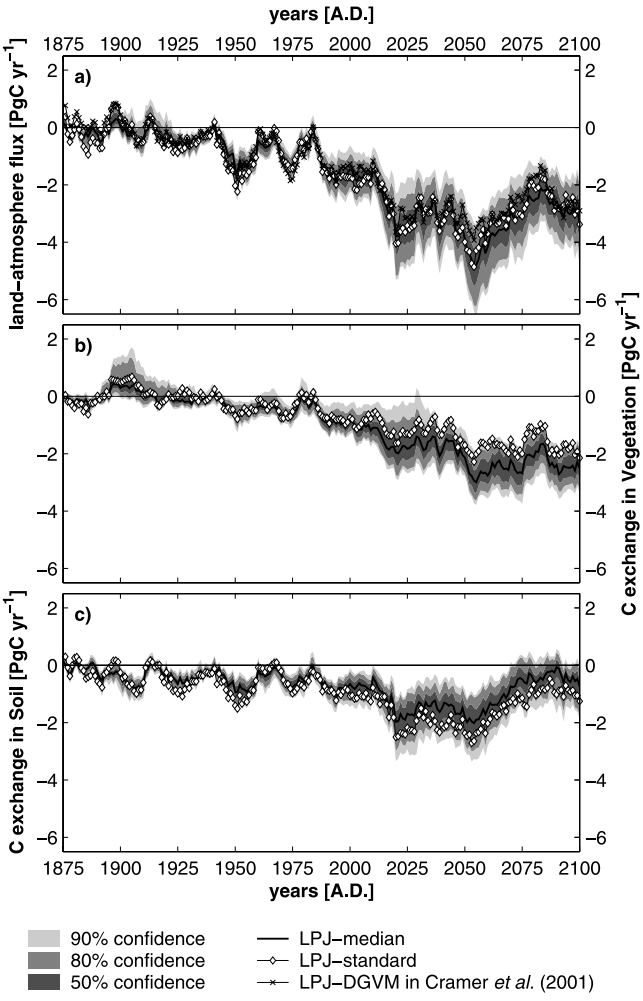

Figure 5. Global land-atmosphere flux (10-year running average, PgC yr^{-1}) under the IS92a HadCM2-SUL climate change scenario: (a) land-atmosphere flux, (b) C exchange of the vegetation, and (c) C exchange of SOM pools. See color version of this figure at back of this issue.

agreement with the results of *Cramer et al.* [2001]. This effect can be attributed to a strong decline in precipitation over the tropics, a particular feature of the climate scenario used in this study. In the northern extra tropics, where the strongest climate change is simulated under this scenario, C sequestration is still substantial by the end of the twenty-first century, but there is considerable uncertainty associated equally with soil and vegetation processes.

[38] Despite the large range of uncertainty in modeled water-stress (a result of varying g_m over a wide range) the expansion of savanna into arid grasslands of the tropics is common to all simulations (Figure 6a). All simulations show an expansion of high latitude forests, as well as an increased deciduousness of temperate and southern boreal forests (Figures 6b and 6c). Most of the vegetation C uptake is located in this area, and its uncertainty controlled by the parameter $f_{sapwood}$, which governs the rate of vegetation C accumulation in newly establishing PFTs. A concurrent decline in precipitation and increase in deciduousness in parts of Southern Africa and America leads to a reduction in *NBP*.

4. Discussion

[39] Of the 36 parameters included in the survey only few have an overriding influence on the modeled terrestrial

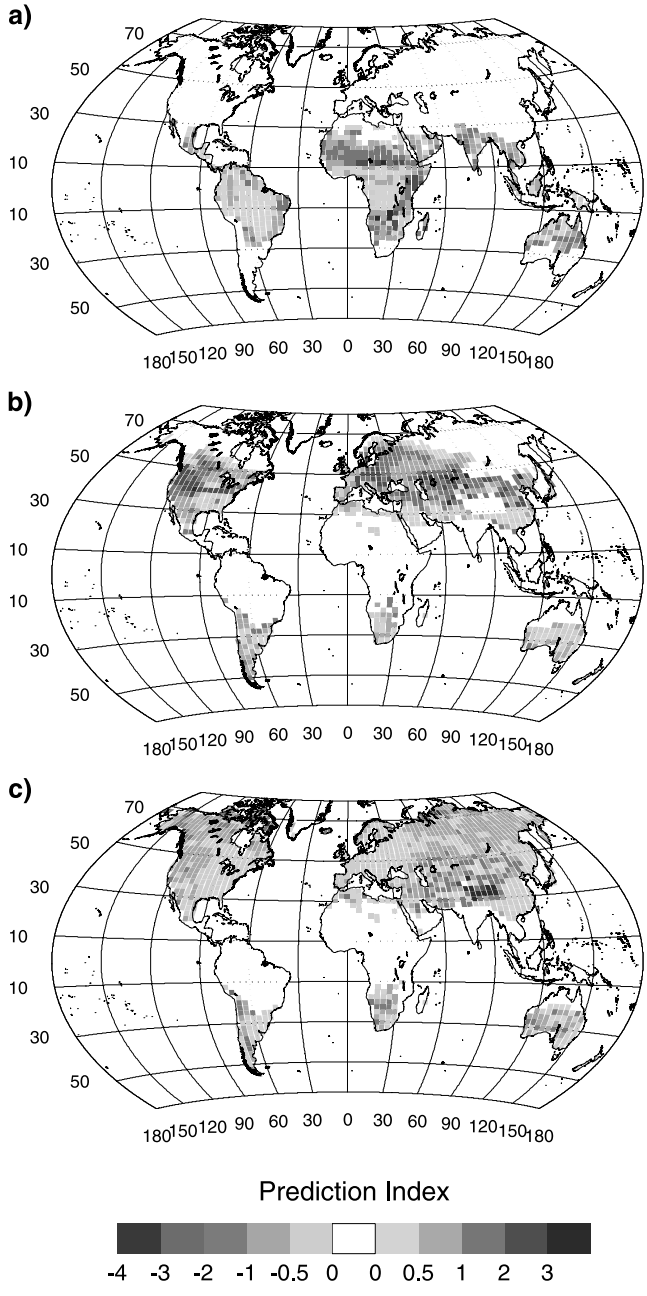

Figure 6. Change in foliage projective coverage between 2000 and 2100 for (a) tropical rain green, (b) temperate deciduous, and (c) temperate herbaceous PFTs; expressed as prediction index, i.e., mean change/standard deviation of change from the uncertainty experiment. An absolute value of >2 indicates a robust model result; typically, trends have similar direction for much lower values. See color version of this figure at back of this issue.

biosphere dynamics. In particular, LPJ-DGVM shows little sensitivity to many of those parameters whose "correct" values, in the absence of suitable measurements, are particularly uncertain, for example, several parameters describing allometry (k_{allom1}, k_{allom2}, k_{allom3}), stand structure (CA_{max}), and fire dynamics (r_{fire}, $fuel_{min}$). Parameters that contribute most to overall model uncertainty are those controlling net assimilation rate and water exchange. This is in general agreement with the results obtained by [*Knorr*, 2000; *Knorr and Heimann*, 2001] for the BETHY model, and [*White et al.*, 2000b] for BIOME-BGC. In particular, only a few parameters are associated with the uncertainty in A at equilibrium, reflecting the big-leaf approach employed in these models.

[40] The uncertainty range of *NPP* is of a similar magnitude to the range among models reported from model intercomparison studies [*Heimann et al.*, 1998; *Cramer et al.*, 2001]. This suggests that these differences might to a large extent be associated with parameter-based uncertainty. Since *NPP* is the major driving force for plant performance and vegetation dynamics, parameters that influence *NPP* have a strong influence on the overall ecosystem dynamics simulated by the model. *NPP* plays the dominant role in determining the sizes of the various C pools in equilibrium, as also noted by *Gerber et al.* [2004].

[41] The range of present-day global land-atmosphere flux estimated in this study may be compared to -0.6 to -3.0 PgC yr^{-1} (1990s) among six DGVMs (including LPJ-DGVM) obtained by *Cramer et al.* [2001] using the same driving data. Model based fluxes in the 1980s range between -1.1 and -2.3 PgC yr^{-1} among four TBMs (likewise including LPJ-DGVM [*McGuire et al.*, 2001]). The "residual terrestrial sink," as inferred from the global C budget, which also accounts for effects on vegetation that are not modeled by LPJ-DGVM such as nitrogen deposition and tropospheric ozone, has been estimated at -0.3 to -4.0 PgC yr^{-1} (1980s) or -1.6 to -4.8 PgC yr^{-1} (1990s) [*House et al.*, 2003]. In the absence of any land-use change that could alter the terrestrial C balance due to deforestation or forest regrowth, the modeled present-day land C uptake is located in roughly equal strength in the tropics (between 20°S and 5°N) and the northern extra tropics, with a particularly strong uptake above 40°N, which is consistent with earlier findings [*Kicklighter et al.*, 1999].

[42] Despite considerable uncertainty in modeled present-day and future net assimilation and primary production, as well as C storage, some robust features are apparent from the scenario analyses. Substantial increases in A because of increased water-use efficiency occurred consistently in all simulations (as noted by *Kicklighter et al.* [1999]), suggesting that alternative parameter values do not change the direction of the process response. All major regional responses of vegetation to changes in climate are simulated consistently for the majority of simulations. Resulting regional patterns of C uptake or loss from vegetation and soil are also consistently modeled, even though the magnitude of the effect is relatively uncertain.

[43] Whereas we evaluated the effect of parameter uncertainty on future responses of the terrestrial biosphere as simulated by one particular DGVM, *Cramer et al.* [2001] assessed uncertainties associated with the different process representations encapsulated by different models (i.e., six DGVMs, one climate scenario), while *Schaphoff et al.* [2005] investigated uncertainties associated with climate change projections produced by different climate models (i.e., one DGVM, five different climate models, all driven with the IS92a emission scenario). Results from the three studies agree well in terms of modern *NPP*, R_h and *NBP*, as well as in inter-annual variability, and the overall decadal trend for the scenario period when forced with the same climate data. Uncertainty in present-day *NBP* is equally large among different DGVMs and results obtained using different parameterizations of one particular model. Under climate change, all three studies point to an initial increase in terrestrial carbon stocks, followed by a decline in net C uptake in the second half of the twenty-first century. The decline of biospheric C uptake, and a potential net C loss toward the end of the twenty-first century are in agreement with other model studies [*Cox et al.*, 2000; *White et al.*, 2000a; *Joos et al.*, 2001; *Dufresne et al.*, 2002; *Friedlingstein et al.*, 2003; *Jones et al.*, 2003]. The uncertainty range in modeled C uptake integrated over the entire twenty-first century in the present study is 201 (117–264) PgC (vegetation) and 107 (32–212) PgC (soil). These ranges compare to 151–340, and 28–220 PgC for vegetation and soil pools, respectively, from the DGVM inter-comparison [*Cramer et al.*, 2001], and to 0–150 PgC (vegetation) and -70 to 41 PgC (soils) for four different climate scenarios (excluding the older HadCM2 scenario [*Schaphoff et al.*, 2005]). In all three studies, models predict a trend toward increased *NPP* and vegetation growth as response to increased atmospheric CO_2 and temperature, particularly at high northern latitudes, concurrent with an expansion of boreal forests. This trend is consistently modeled among different DGVMs, future climate scenarios and model parameterizations. Strong regional differences in changes of vegetation composition were, however, observed for tropical regions among different climate scenarios, mainly as a result of different regional changes in precipitation [*Schaphoff et al.*, 2005]. The present study shows that simulated shifts in dominant vegetation types, regional patterns of *NBP* and their change over time are relatively robust to the choice of model parameterization.

[44] We applied a relatively simple method to constrain the parameter-based model uncertainty in an attempt to approach a realistic uncertainty range for modeled present-day and potential future *NBP*, as well as to demonstrate the effect of parameter-based uncertainty on modeling terrestrial biosphere dynamics. A more sophisticated method of constraining distribution functions for model output variables, assigning a probability to results from each model run based on the distance between the run and the "best-guess" region of a particular benchmark, was tested for the present-day analysis. However, results were similar to those obtained using the simpler approach, and would not greatly affect the conclusions of our study.

[45] The obvious starting point to reduce parameter-based uncertainty would be to constrain *NPP* directly from

observations, because of the importance of *A* and *NPP* in global vegetation models. As detailed in section 3.3.1, currently available *NPP* measurements are probably insufficient for this purpose. C flux estimates from eddy-covariance measurements that integrate C and H_2O fluxes at the ecosystem scale offer some potential to constrain the parameter space using inverse methods [*Wang et al.*, 2001; *Reichstein et al.*, 2003; *Knorr and Kattge*, 2005]. α_{C3} and α_a contribute most to the uncertainty in the modeled seasonal cycle by amplifying its magnitude. However, the importance of these parameters in determining monthly *NEE* were in most cases strongly anti-correlated with r_{growth}, r_{maint}, and r_{ea}. This implies that a particular modeled seasonal cycle of *NEE* might be obtained from a multitude of combinations of these parameters, such that these parameters might be difficult to constrain based on net C fluxes. Partitioning the net flux into uptake and respiratory components could potentially help to identify parameter contributions, especially for respiratory processes [*Wang et al.*, 2001]. However, large uncertainty still exists with respect to the correct flux separation [*Janssens et al.*, 2001; *Ogee et al.*, 2004]. Parameter correlations could, however, be derived by constraining model results with flux data and thus reducing the parameter space [*Knorr and Kattge*, 2005]. The findings of the present study demonstrate clearly that parameter importance varies between different sites. A representative collection of high quality seasonal *NEE* data sets for all major biomes would thus allow uncertainty in global terrestrial modeling to be reduced.

[46] Measurements of the seasonal variations of atmospheric CO_2 concentrations integrate carbon fluxes over larger regions; hence they have the potential to avoid spatial bias. The largest reduction in absolute error may be obtained in the northern latitudes, where the seasonal cycle appears to be most strongly controlled by light-use efficiency effects on vegetation productivity. Atmospheric inversion studies likewise point to light-use efficiency as a major controlling factor for seasonal variation in CO_2 exchange [*Kaminski et al.*, 2002; *Still et al.*, 2004]. However, uncertainty about the influence of the co-occurring fluxes of anthropogenic and oceanic origin, atmospheric transport fields used to map emissions of the terrestrial biosphere to the CO_2 monitoring stations, and data availability and quality [*Rayner et al.*, 2005] limit the degree to which uncertainty in parameter values can be effectively reduced.

[47] Both, eddy-covariance and CO_2 measurements could potentially be used to constrain parameters that govern short-term ecosystem processes (e.g., α_{C3}, α_a, θ, r_{growth}). These parameters contribute most to the parameter-based uncertainty in present-day *NEE*, and amplify the rate of *A* and *NPP* increase as a response to future climate scenarios. However, in our global change case study these parameters contribute to only 4% and 45% of the uncertainty in C uptake by vegetation and soil, respectively. Transient projections of climate change effects on vegetation C storage are influenced to a much greater extent by uncertainty in vegetation dynamics, primarily the rate at which forests can accumulate C after disturbance, or in response to changing environmental conditions. Similarly, uncertainty in modeled SOM change, although showing a strong influence of uncertainty in litter fall, is strongly linked to parameters governing the average turnover time of the SOM pools, particularly in regions in which soils become a source of CO_2 in the future in these scenario analyses. These results highlight the need for improved understanding of the response of SOM to changing environmental conditions [e.g., *Fang et al.*, 2005; *Knorr et al.*, 2005], as well as for improved understanding of potential changes in the competitive balance between PFTs under climate change.

[48] We evaluated parameter importance for average present-day conditions, and constrained the parameter space further using present-day observations of the global C cycle. Parameters that appear of little importance in this approach may still have substantial impact on model simulations under other than present-day conditions. For instance, *Fang et al.* [2005] showed that uncertainty in the apparent Q_{10} of soil respiration could lead to an up to 70% difference in projected soil C losses under future climate change in temperate regions. *Joos et al.* [2001], using LPJ-DGVM, demonstrated that cumulative land-atmosphere fluxes (2000–2100) differed by 188 PgC depending on whether soil respiration was assumed to be temperature dependent (Lloyd-Taylor) or not. Uncertainty in soil C changes through the twenty-first century, as simulated in this study, is of a comparable magnitude, but associated with different parameters: The rate parameter in the Lloyd-Taylor equation was found not to be important in determining present-day C cycling, and was thus not included in estimating the uncertainty in the future C balance. Data assimilation, as discussed above, may improve the identification of parameters that are of importance also under changing environmental conditions. However, these methods rely on present-day observations to test model performance [e.g., *Rayner et al.*, 2005], which still might be insufficient to reduce uncertainty of the long-term response of some terrestrial processes, for example, the long-term responses of photosynthesis to enhanced [CO_2], or soil respiration to global warming. Uncertainties due to gaps in process understanding and uncertainties in associated with alternative process formulations at scales relevant to global terrestrial biosphere modeling [*Knorr and Heimann*, 2001] are important, but beyond the scope of the present study.

[49] The uncertainty range of a particular model output variable depends on the choice of distribution function for the parameters in question. We choose to apply the principle of parsimony in assuming a uniform distribution function for all but one parameter. An alternative choice would be a bell-shaped function or similar, simulating parameter values distal from the mean of "best guess" values with reduced probability. This would tend to reduce the spread in model results, giving a more conservative estimate of the potential model uncertainty. Some parameters are likely to co vary in nature, whereas they were assumed, with one exception, to vary independently in our study; again, our approach is likely to overestimate rather than to underestimate the true uncertainty range.

[50] The exact ranking of the uncertainty contribution of individual parameters, or their functional equivalents in

other models, will be influenced by the structure of the particular model under investigation. Nevertheless, LPJ-DGVM may be considered exemplary for the DGVM family of models. These models generally follow similar approaches to simulate plant C and H_2O exchanges with the atmosphere. Certain parameter groups, for instance those controlling the light-use efficiency of photosynthesis at the ecosystem scale, will very likely play a pivotal role in model uncertainty for any DGVM, due to the central role of NPP in determining vegetation structure and dynamics. The methodology presented here could be readily applied to other models to further corroborate our findings.

[51] This study focuses on the uncertainty in process-based terrestrial biosphere models due to imperfect knowledge (or implicit uncertainty) of the "correct" parameter values used in scaled representations of ecosystem processes, and aims at providing quantitative information about the confidence that can be placed in model results. However, other aspects of model uncertainty were not addressed; for example, uncertainty due to incomplete knowledge of the true mechanisms underlying certain ecosystem phenomena, as well as uncertainty in the driving environmental data, which may be equally important [e.g., *Knorr and Heimann*, 2001]. Future steps toward a quantitative assessment of the uncertainty in modeling terrestrial biosphere dynamics will need to account for uncertainty related to model assumptions, for example, the equilibrium of C cycle at the beginning of the twenty-first century, and to consider driving factors other than climate and atmospheric CO_2 change, such as land-use change [*McGuire et al.*, 2001] and N deposition [*Vitousek et al.*, 1997]. It should be noted that model robustness does not necessarily imply that model predictions are correct. In fact, model failure to correctly predict observations considering model uncertainty can point to areas in which model improvements are required. Better evaluation data and improved process understanding, for example, of the response of ecosystem to disturbances, are indispensable for the reliable modeling of the terrestrial biosphere.

5. Conclusions

[52] We presented an assessment of parameter-based uncertainty in modeling the present-day and future terrestrial biosphere dynamics using one particular DGVM. Of the 36 parameters in our survey, only a limited subset of parameters is associated with most of the present-day model uncertainty. An improved understanding of the scaling of leaf-level photosynthesis to ecosystems, the hydraulic coupling of vegetation and atmosphere and plant respiration processes appear to be the most important priorities to reduce parameter-based uncertainty in the modeling of present-day ecosystem C cycling. The rate of C accumulation in vegetation and the turnover time of SOM were identified as major contributors to uncertainty in future C balance estimates, highlighting the need for more appropriate experiments and better validation data sets to improve model performance.

[53] The substantial uncertainty range in *NPP* in this study is of a similar magnitude to the range observed between different DGVMs and other model-based estimates of global *NPP*. Uncertainty propagation leads to considerable uncertainty in sizes of C pools. Soil C pools, due to their long turnover times, represent the most uncertain model outputs. Despite this, contemporary global vegetation distribution and land-atmosphere flux are relatively robust model results. The overall response of LPJ-DGVM to a particular climatic forcing is maintained among most of the alternative parameterizations tested in this study. In particular, the response of vegetation to increased levels of CO_2, shifts in vegetation patterns as a result of climate change, and the effect of global warming on SOM pools are reasonably robust model results. In effect, long-term trends in global land-atmosphere fluxes are reliably modeled, although uncertainty range reaches -3.35 ± 1.45 PgC yr^{-1} by the end of the twenty-first century under the particular climate scenario used in this study. On the basis of our analysis we recommend that uncertainty analyses should be an integral part of the development and validation process for all process-oriented ecosystem models.

[54] **Acknowledgments.** The authors are grateful to Stefano Tarantola (JRC, Italy) for kindly providing the software tool SimLab to generate the Latin hypercube samples and to Christoph Müller (PIK) for providing the aggregated 3.0° CRU climatology. We also thank Kathrin Poser, Wolfgang Cramer, Markus Reichstein and two anonymous reviewers for helpful comments on earlier versions of this manuscript. S. Z. acknowledges funding from the HSP Brandenburg (AZ: 24-04/323;200). B. S. acknowledges funding through the Swedish Research Council for Environment, Agriculture Sciences and Spatial Planning. The study was part of the Advanced Terrestrial Ecosystem Analysis and Modeling (ATEAM) initiative (EVK2-2000-00075) of the fifth European Community Framework Programme.

References

Andreae, M. O., and P. Merlet (2001), Emission of trace gases and aerosols from biomass burning, *Global Biogeochem. Cycles*, *15*(4), 955–966.

Beringer, J., S. McIlwaine, A. H. Lynch, F. S. Chapin, and G. B. Bonan (2002), The use of a reduced form model to assess the sensitivity of a land surface model to biotic surface parameters, *Clim. Dyn.*, *19*, 455–466.

Campolongo, F., J. Kleijnen, and T. Andres (2000), Screening Methods, in *Sensitivity Analysis*, edited by A. Saltelli, K. Chan, and E. M. Scott, pp. 65–80, John Wiley, Hoboken, N. J.

Ciais, P., et al. (1997), A three-dimensional synthesis study of delta O-18 in atmospheric CO_2: 1. Surface fluxes, *J. Geophys. Res.*, *102*(D5), 5857–5872.

Clark, D. A., S. Brown, D. W. Kicklighter, J. Q. Chambers, J. R. Thomlinson, and J. Ni (2001), Measuring net primary production in forests: concepts and field methods, *Ecol. Appl.*, *11*(2), 356–370.

Cox, P. M., R. A. Betts, C. D. Jones, S. A. Spall, and I. J. Totterdell (2000), Acceleration of global warming due to carbon-cycle feedbacks in a coupled climate model, *Nature*, *408*(6813), 750.

Cramer, W., D. W. Kicklighter, A. Bondeau, B. Moore, C. Churkina, B. Nemry, A. Ruimy, and A. L. Schloss (1999), Comparing global models of terrestrial net primary productivity (NPP): Overview and key results, *Global Change Biol.*, *5*, 1–15.

Cramer, W., et al. (2001), Global response of terrestrial ecosystem structure and function to CO_2 and climate change: Results from six dynamic global vegetation models, *Global Change Biol.*, *7*, 357–373.

Daly, C., D. Bachelet, J. M. Lenihan, R. P. Neilson, W. Parton, and D. Ojima (2000), Dynamic simulation of tree-grass interactions for global change studies, *Ecol. Appl.*, *10*(2), 449–469.

Dargaville, R. J., et al. (2002), Evaluation of terrestrial carbon cycle models with atmospheric CO_2 measurements: Results from transient simulations considering increasing CO_2, climate, and land-use effects, *Global Biogeochem. Cycles*, *16*(4), 1092, doi:10.1029/2001GB001426.

Dufresne, J. L., P. Friedlingstein, M. Berthelot, L. Bopp, P. Ciais, L. Fairhead, H. Le Treut, and P. Monfray (2002), On the magnitude of positive feedback between future climate change and the carbon cycle, *Geophys. Res. Lett.*, *29*(10), 1405, doi:10.1029/2001GL013777.

Fang, C., P. Smith, J. Moncrieff, and J. Smith (2005), Similar response of labile and resistant organic matter pools to changes in temperature, *Nature*, *433*, 57–58.

Foley, J. A., I. C. Prentice, N. Ramankutty, S. Levis, D. Pollard, S. Sitch, and A. Haxeltine (1996), An integrated biosphere model of land surface processes, terrestrial carbon balance, and vegetation dynamics, *Global Biogeochem. Cycles*, *10*(4), 603–628.

Food and Agriculture Organization of the U.N. (1991), *The Digitized Soil Map of the World (Release 1.0)*, Rome.

Friedlingstein, P., J. L. Dufresne, P. M. Cox, and P. Rayner (2003), How positive is the feedback between climate change and the carbon cycle?, *Tellus, Ser. B*, *55*(2), 692–700.

Friend, A. D., A. K. Stevens, R. G. Knox, and M. G. R. Cannell (1997), A process-based, terrestrial biosphere model of ecosystem dynamics (Hybrid v3.0), *Ecol. Modell.*, *95*(2–3), 249–287.

Gerber, S., F. Joos, and C. Prentice (2004), Sensitivity of a dynamic global vegetation model to climate and atmospheric CO_2, *Global Change Biol.*, *10*, 1223–1239.

Gerten, D., S. Schaphoff, U. Haberlandt, W. Lucht, and S. Sitch (2004), Terrestrial vegetation and water balance—Hydrological evaluation of a dynamic global vegetation model, *J. Hydrol.*, *286*(1–4), 249–270.

GLOBALVIEW-CO_2 (1999), Cooperative Atmospheric Data Integration Project—Carbon Dioxide [CD-ROM], Clim. Monit. and Diag. Lab., Boulder, Colo.

Hallgren, W. S., and A. J. Pitman (2000), The uncertainty in simulations by a global biome model (BIOME3) to alternative parameter values, *Global Change Biol.*, *6*, 483–495.

Haxeltine, A., and I. C. Prentice (1996a), BIOME3: An equilibrium terrestrial biosphere model based on ecophysiological constraints, resource availability, and competition amongst plant functional types, *Global Biogeochem. Cycles*, *10*(4), 693–709.

Haxeltine, A., and I. C. Prentice (1996b), A general model for the light use efficiency of primary production, *Funct. Ecol.*, *10*, 551–561.

Heimann, M., et al. (1998), Evaluation of terrestrial carbon cycle models through simulations of the seasonal cycle of atmospheric CO_2: First results of a model intercomparison study, *Global Biogeochem. Cycles*, *12*(1), 1–24.

Helton, J., and F. Davis (2000), Sampling-based methods, in *Sensitivity Analysis*, edited by A. Saltelli, K. Chan, and E. M. Scott, pp. 101–153, John Wiley, Hoboken, N. J.

Houghton, R. A., and D. L. Skole (1990), Carbon-transformation of the global environment, in *The Earth as Transformed by Human Action—Global and Regional Changes in the Biosphere Over the Past 300 Years*, edited by B. L. Turner et al., pp. 393–408, Cambridge Univ. Press, New York.

House, J. I., I. C. Prentice, N. Ramankutty, R. A. Houghton, and M. Heimann (2003), Reconciling apparent inconsistencies in estimates of terrestrial CO_2 sources and sinks, *Tellus, Ser. B*, *55*(2), 345–363.

Iman, R. L., and W. Conover (1982), A distribution free approach to inducing rank correlation among input variables, *Commun. Stat. B*, *11*, 311–334.

Intergovernmental Panel on Climate Change (1992), *Climate Change 1992: The Supplementary Report to the IPCC Scientific Assessment*, edited by J. T. Houghton, B. A. Callender, and S. K. Varney, Cambridge Univ. Press, New York.

Intergovernmental Panel on Climate Change (2001), *Climate Change 2001: The Scientific Basis. Contribution of Working Group I to the Third Assessment Report of the Intergovernmental Panel on Climate Change*, edited by J. T. Houghton et al., 881 pp., Cambridge Univ. Press, New York.

Janssens, I. A., et al. (2001), Productivity overshadows temperature in determining soil and ecosystem respiration across European forests, *Global Change Biol.*, *7*(3), 269–278.

Johns, T. C., R. E. Carnell, J. F. Crossley, J. M. Gregory, J. F. B. Mitchell, C. A. Senior, S. F. B. Tett, and R. A. Wood (1997), The second Hadley Centre coupled ocean-atmosphere GCM: Model description, spinup and validation, *Clim. Dyn.*, *13*, 103–134.

Jones, C. D., P. M. Cox, R. L. H. Essery, D. L. Roberts, and M. J. Woodage (2003), Strong carbon cycle feedbacks in a climate model with interactive CO_2 and sulphate aerosols, *Geophys. Res. Lett.*, *30*(9), 1479, doi:10.1029/2003GL016867.

Joos, F., I. C. Prentice, S. Sitch, R. Meyer, G. Hooss, G. K. Plattner, S. Gerber, and K. Hasselmann (2001), Global warming feedbacks on terrestrial carbon uptake under the Intergovernmental Panel on Climate Change (IPCC) emission scenarios, *Global Biogeochem. Cycles*, *15*(4), 891–907.

Kaminski, T., M. Heimann, and R. Giering (1999a), A coarse grid three-dimensional global inverse model of the atmospheric transport: 1. Adjoint model and Jacobian matrix, *J. Geophys. Res.*, *104*(D15), 18,535–18,553.

Kaminski, T., M. Heimann, and R. Giering (1999b), A coarse grid three-dimensional global inverse model of the atmospheric transport: 2. Inversion of the transport of CO_2 in the 1980s, *J. Geophys. Res.*, *104*(D15), 18,555–18,581.

Kaminski, T., W. Knorr, P. J. Rayner, and M. Heimann (2002), Assimilating atmospheric data into a terrestrial biosphere model: A case study of the seasonal cycle, *Global Biogeochem. Cycles*, *16*(4), 1066, doi:10.1029/2001GB001463.

Kicklighter, D. W., et al. (1999), A first-order analysis of the potential role of CO_2 fertilization to affect the global carbon budget: A comparison of four terrestrial biosphere models, *Tellus, Ser. B*, *51*(2), 343–366.

Kindermann, J., G. Würth, G. Kohlmaier, and F. W. Badeck (1996), Interannual variation of carbon exchange fluxes in terrestrial ecosystems, *Global Biogeochem. Cycles*, *10*(4), 737–755.

Kleijnen, J. (1998), Experimental design for sensitivity analysis, optimization and validation of simulation models, in *Handbook of Simulation—Principles, Methodology, Advances, Applications, and Practice*, edited by J. Banks, pp. 173–224, John Wiley, Hoboken, N. J.

Knorr, W. (2000), Annual and interannual CO_2 exchanges of the terrestrial biosphere: Process-based simulations and uncertainties, *Global Ecol. Biogeogr.*, *9*, 225–252.

Knorr, W., and M. Heimann (1995), Impact of drought stress and other factors on seasonal land biosphere co_2 exchange studied through an atmospheric tracer transport model, *Tellus, Ser. B*, *47*(4), 471–489.

Knorr, W., and M. Heimann (2001), Uncertainties in global terrestrial biosphere modeling: 1. A comprehensive sensitivity analysis with a new photosynthesis and energy balance scheme, *Global Biogeochem. Cycles*, *15*(1), 207–225.

Knorr, W., and J. Kattge (2005), Inversion of Terrestrial Ecosystem Parameter Values against Eddy Covariance Measurements by Monte Carlo Sampling, *Global Change Biol.*, in press.

Knorr, W., I. C. Prentice, J. House, and E. Holland (2005), Long-term sensitivity of soil carbon turnover to warming, *Nature*, *433*, 298–301.

Knutti, R., T. F. Stocker, F. Joos, and G.-K. Plattner (2002), Constraints on radiative forcing and future climate change from observations and climate model ensembles, *Nature*, *416*, 719–723.

Kolari, P., J. Pumpanen, U. Rannik, H. Ilvesniemi, P. Hari, and F. Berninger (2004), Carbon balance of different aged Scots pine forests in Southern Finland, *Global Change Biol.*, *10*, 1106–1119.

Maayar, M., D. T. Price, T. A. Black, E. R. Humphreys, and E.-M. Jork (2002), Sensitivity tests of the Integrated Biosphere Simulator to soil and vegetation characteristics in a Pacific coastal coniferous forest, *Atmos. Ocean*, *40*(3), 313–332.

McGuire, A. D., J. M. Melillo, J. T. Randerson, W. J. Parton, M. Heimann, R. A. Meier, J. S. Clein, D. W. Kicklighter, and W. Sauf (2000), Modeling the effects of snowpack on heterotrophic respiration across northern temperate and high latitude regions: Comparison with measurements of atmospheric carbon dioxide in high latitudes, *Biogeochemistry*, *48*(1), 91–114.

McGuire, A. D., et al. (2001), Carbon balance of the terrestrial biosphere in the twentieth century: Analyses of CO_2, climate and land use effects with four process-based ecosystem models, *Global Biogeochem. Cycles*, *15*(1), 183–206.

McKay, M., R. Beckman, and W. Conover (1979), A comparison of three methods of selecting values of input variables in the analysis of output from a computer code, *Technometrics*, *21*, 239–245.

Melillo, J. M., et al. (1995), Vegetation Ecosystem Modeling and Analysis Project: Comparing biogeography and biogeochemistry models in a continental-scale study of terrestrial ecosystem responses to climate-change and CO_2 doubling, *Global Biogeochem. Cycles*, *9*(4), 407–437.

Mitchell, J., T. Johns, J. Gregory, and S. Tett (1995), Climate responses to increasing levels of greenhouse gases and sulphate aerosols, *Nature*, *376*, 501–504.

Mitchell, T. D., T. R. Carter, P. D. Jones, M. Hulme, and M. New (2004), A comprehensive set of high-resolution grids of monthly climate for Europe and the globe: The observed record (1901–2000) and 16 scenarios (2001–2100), *Work. Pap. 55*, 33 pp., Tyndall Cent. for Clim. Change Res., Univ. of East Anglia, Norwich, UK.

Ogee, J., P. Peylin, M. Cuntz, T. Bariac, Y. Brunet, P. Berbigier, P. Richard, and P. Ciais (2004), Partitioning net ecosystem carbon exchange into net assimilation and respiration with canopy-scale isotopic measurements: An error propagation analysis with (CO_2)-C-13 and (COO)-O-18 data, *Global Biogeochem. Cycles*, *18*(2), GB2019, doi:10.1029/2003GB002166.

Post, W. M., A. W. King, and S. D. Wullschleger (1997), Historical variations in terrestrial biospheric carbon storage, *Global Biogeochem. Cycles*, *11*(1), 99–109.

Prentice, I. C., W. Cramer, S. P. Harrison, R. Leemans, R. A. Monserud, and A. M. Solomon (1992), A global biome model based on plant physiology and dominance, soil properties and climate, *J. Biogeogr.*, *19*(2), 117–134.

Prentice, I. C., M. Heimann, and S. Sitch (2000), The carbon balance of the terrestrial biosphere: Ecosystem models and atmospheric observations, *Ecol. Appl.*, *10*(6), 1553–1573.

Prentice, I., G. Farquhar, M. Fasham, M. Goulden, M. Heimann, V. Jaramillo, H. Kheshgi, C. Le Quéré, R. Scholes, and D. Wallace (2001), The carbon cycle and atmospheric carbon dioxide, in *Climate Change 2001: The Scientific Basis—Contribution of Working Group I to the Third Assessment Report of the Intergovernmental Panel on Climate Change*, edited by J. T. Houghton et al., pp. 183–237, Cambridge Univ. Press, New York.

Randerson, J., et al. (2002), Carbon isotope discrimination of arctic and boreal biomes inferred from remote atmospheric measurements and a biosphere-atmosphere model, *Global Biogeochem. Cycles*, *16*(3), 1028, doi:10.1029/2001GB001435.

Rayner, P. J., M. Scholze, W. Knorr, T. Kaminski, R. Giering, and H. Widmann (2005), Two decades of terrestrial carbon fluxes from a carbon cycle data assimilation system (CCDAS), *Global Biogeochem. Cycles*, *19*, GB2026, doi:10.1029/2004GB002254.

Reich, P. B., M. B. Walters, and D. S. Ellsworth (1992), Leaf life-span in relation to leaf, plant, and stand characteristics among diverse ecosystems, *Ecol. Monogr.*, *62*(3), 365–392.

Reichstein, M., J. Tenhunen, O. Roupsard, J.-M. Ourcival, S. Rambal, F. Miglietta, A. Peresotti, M. Pecchiari, G. Tirone, and R. Valentini (2003), Inverse modeling of season drought effects of canopy CO_2/H_2O exchange in three Mediterranean ecosystems, *J. Geophys. Res.*, *108*(D23), 4726, doi:10.1029/2003JD003430.

Saltelli, A., K. Chan, and E. M. Scott (2000), *Sensitivity Analysis*, edited by V. Barnett, 486 pp., John Wiley, Hoboken, N. J.

Schaphoff, S., W. Lucht, D. Gerten, S. Sitch, W. Cramer, and C. Prentice (2005), Terrestrial biosphere carbon storage under alternative climate projections, *Clim. Change.*, in press.

Scurlock, J., W. Cramer, R. J. Olson, W. J. Parton, and S. D. Prince (1999), Terrestrial NPP: Toward a consistent data set for global model evaluation, *Ecol. Appl.*, *9*(3), 913–919.

Sitch, S., et al. (2003), Evaluation of ecosystem dynamics, plant geography and terrestrial carbon cycling in the LPJ Dynamic Global Vegetation Model, *Global Change Biol.*, *9*, 161–185.

Smith, B., I. C. Prentice, and M. T. Sykes (2001), Representation of vegetation dynamics in the modelling of terrestrial ecosystems: Comparing two contrasting approaches within European climate space, *Global Ecol. Biogeogr.*, *10*, 621–637.

Steffen, W. L., W. Cramer, M. Plöchl, and H. Bugmann (1996), Global vegetation models: Incorporating transient changes to structure and composition, *J. Veg. Sci.*, *7*, 321–328.

Still, C. J., J. T. Randerson, and I. Y. Fung (2004), Large-scale plant light-use efficiency inferred from the seasonal cycle of atmospheric CO_2, *Global Change Biol.*, *10*, 1240–1252.

Thornton, P. E., et al. (2002), Modeling and measuring the effects of disturbance history and climate on carbon and water budgets in evergreen needleleaf forests, *Agric. For. Meteorol.*, *113*(1–4), 185–222.

Valentini, R., et al. (2000), The Euroflux dataset 2000, in *Carbon, Water and Energy Exchanges of European Forests*, edited by R. Valentini, pp. 1–30, Springer, New York.

Vitousek, P. M., J. D. Aber, R. W. Howarth, G. E. Likens, P. A. Matson, D. W. Schindler, W. H. Schlesinger, and D. G. Tilman (1997), Human alteration of the global nitrogen cycle: Sources and consequences, *Ecol. Appl.*, *7*(3), 737–750.

Wang, Y.-P., R. Leuning, H. A. Cleugh, and P. A. Coppin (2001), Parameter estimation in surface exchange models using nonlinear inversion: how many parameters can we estimate and which measurements are most useful?, *Global Change Biol.*, *7*, 495–510.

White, A., M. G. R. Cannell, and A. D. Friend (2000a), CO_2 stabilization, climate change and the terrestrial carbon sink, *Global Change Biol.*, *6*, 817–833.

White, M. A., P. E. Thornton, S. Running, and R. Nemani (2000b), Parameterization and Sensitivity analysis of the BIOME-BGC Terrestrial Ecosystem Model: Net primary production controls, *Earth Interact.*, *4*, 1–55.

Woodward, F. I., T. M. Smith, and W. R. Emanuel (1995), A global land primary productivity and phytogeography model, *Global Biogeochem. Cycles*, *9*(4), 471–490.

Zobler, L. (1986), A world soil file for global climate modelling, *NASA Tech. Memo.*, *87802*, 32 pp.

F. Hatterman and S. Zaehle, Potsdam Institute for Climate Impact Research (PIK), Department of Global Change and Natural Systems, P.O. Box 60 12 0, D-14412 Potsdam, Germany. (zaehle@pik-potsdam.de)

S. Sitch, Met Office (JCHMR), Crowmarsh-Gifford, Wallingford, OX10 8BB, UK.

B. Smith, Geobiosphere Science Centre, Physical Geography and Ecosystems Analysis, Lund University, Sölvegatan 12, S-22362 Lund, Sweden.

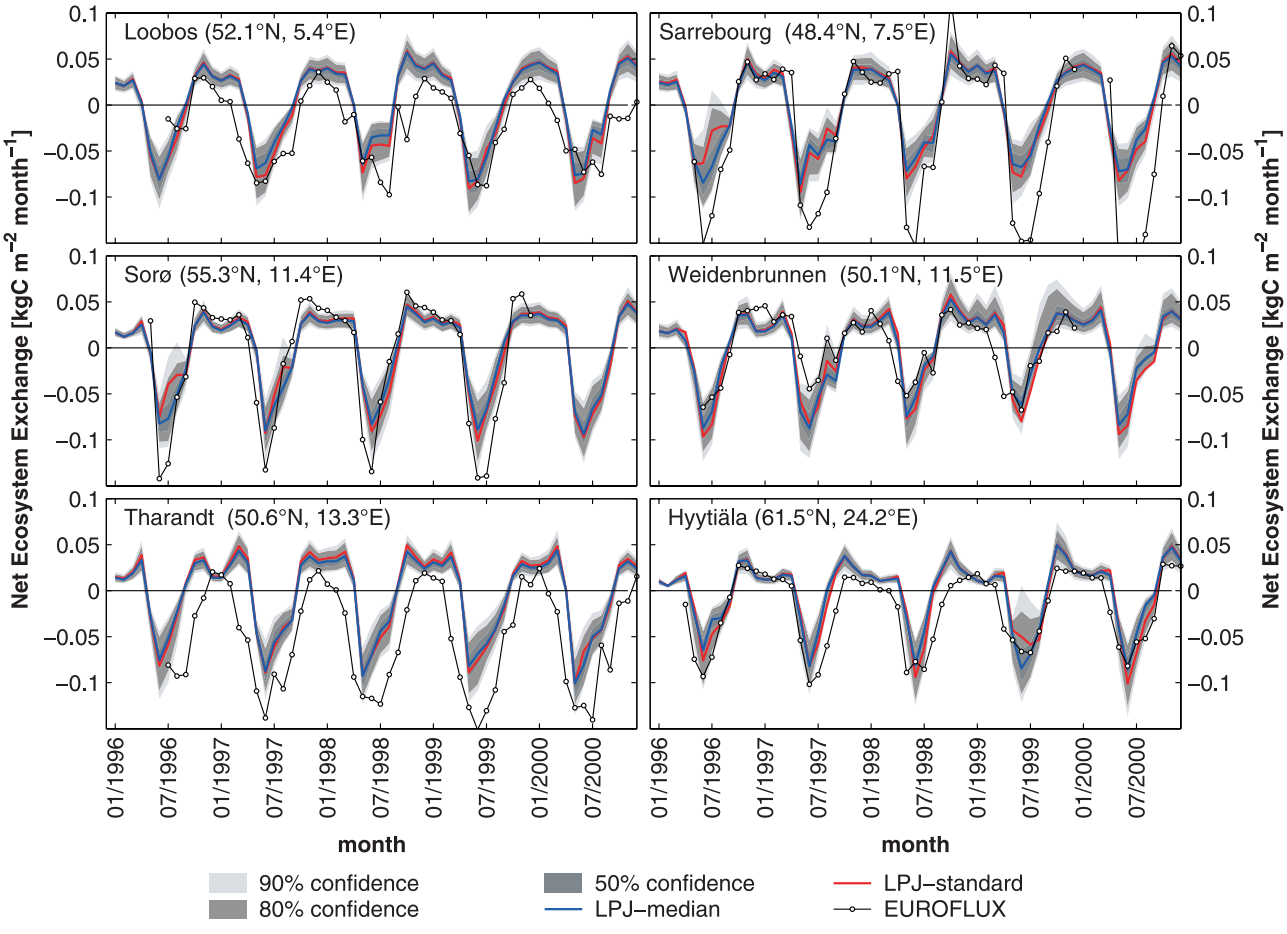

Figure 3. Simulated and observed net ecosystem exchange (*NEE*, kgC m^{-2} $month^{-1}$) for 1996–2000 at six eddy-covariance sites of the EUROFLUX network. Data are taken from *Valentini et al.* [2000]. Statistics are available in auxiliary Table 4.

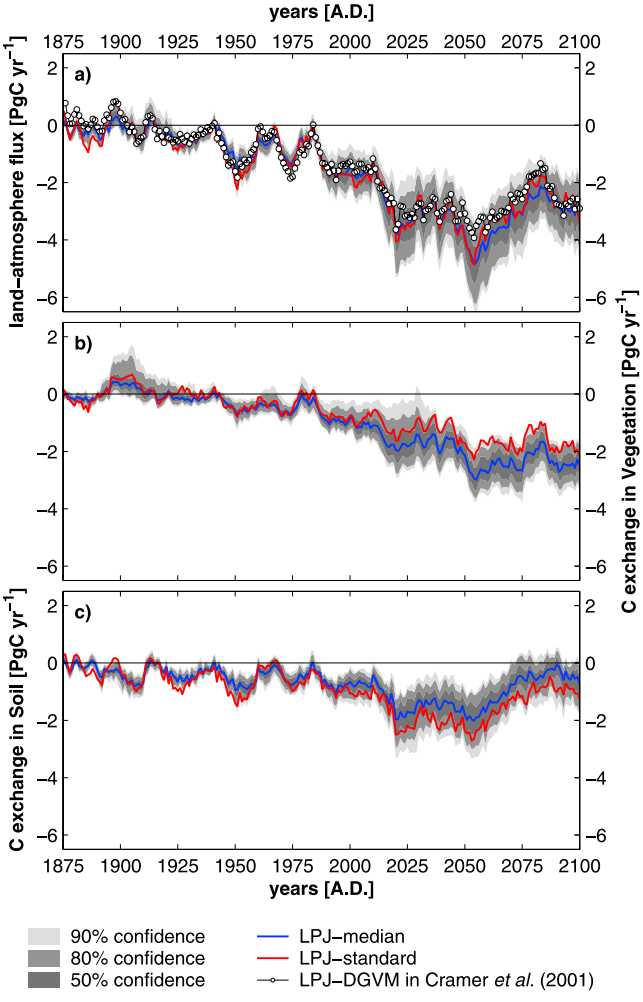

Figure 5. Global land-atmosphere flux (10-year running average, PgC yr^{-1}) under the IS92a HadCM2-SUL climate change scenario: (a) land-atmosphere flux, (b) C exchange of the vegetation, and (c) C exchange of SOM pools.

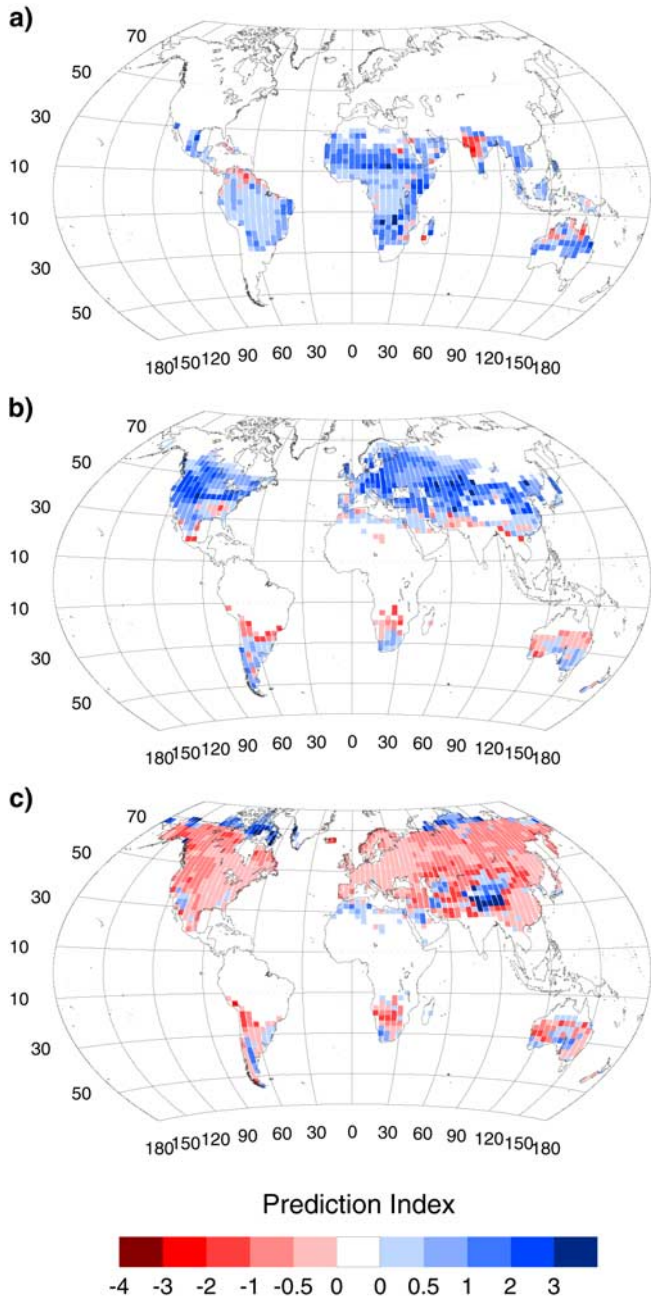

Figure 6. Change in foliage projective coverage between 2000 and 2100 for (a) tropical rain green, (b) temperate deciduous, and (c) temperate herbaceous PFTs; expressed as prediction index, i.e., mean change/standard deviation of change from the uncertainty experiment. An absolute value of >2 indicates a robust model result; typically, trends have similar direction for much lower values.